Dark matter annihilation signals from simulated dwarf spheroidal galaxies

Nassim Bozorgnia

UNIVERSITY OF ALBERTA

2024 CAP Congress, Western University
30 May 2024

Canada Research Chairs
Chaires de recherche du Canada

NSERC
CRSNG

Indirect dark matter searches

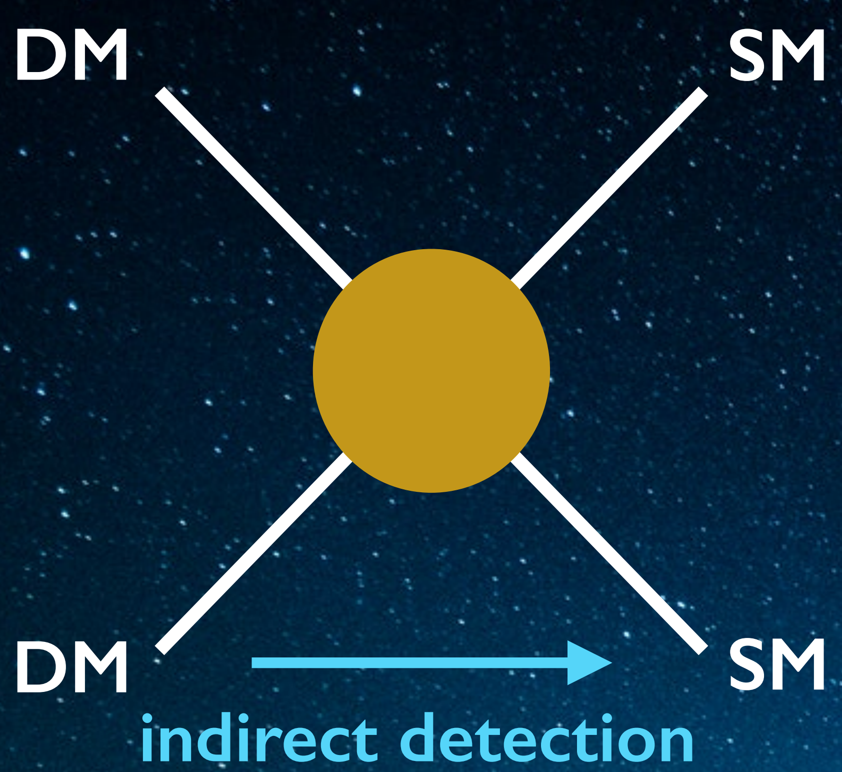

Indirect dark matter searches

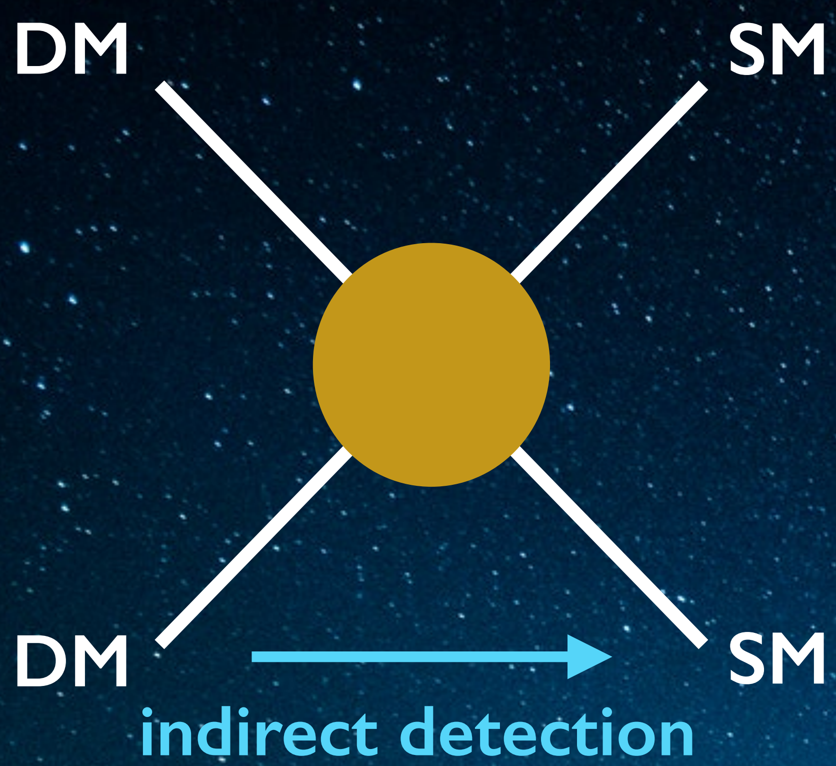

- Need to identify environments of high dark matter (DM) density.

Indirect dark matter searches

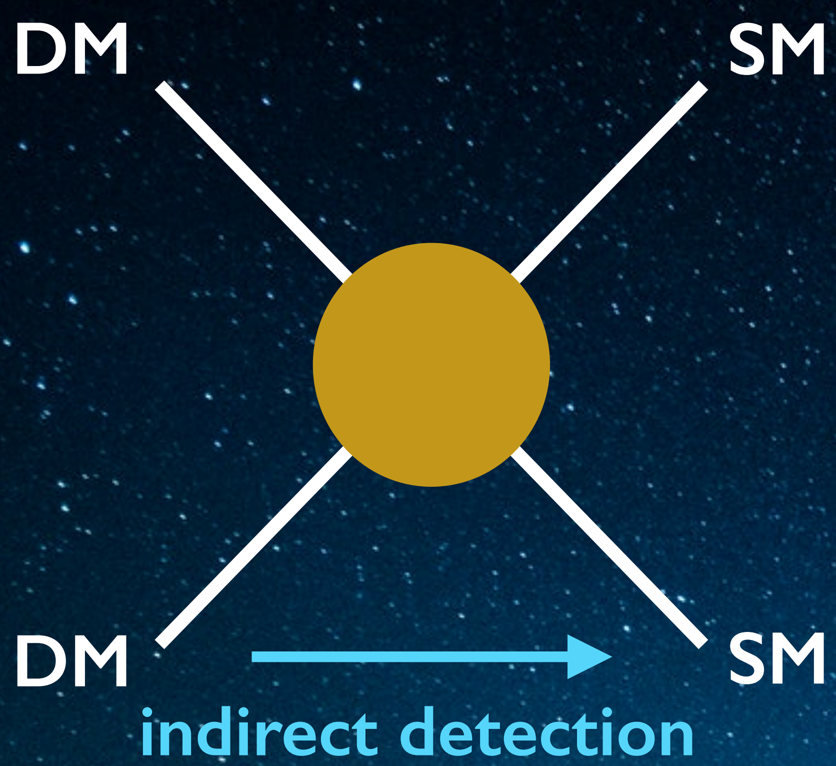

- Need to identify environments of high dark matter (DM) density.
- Signals strongly depend on the DM distribution in these environments.

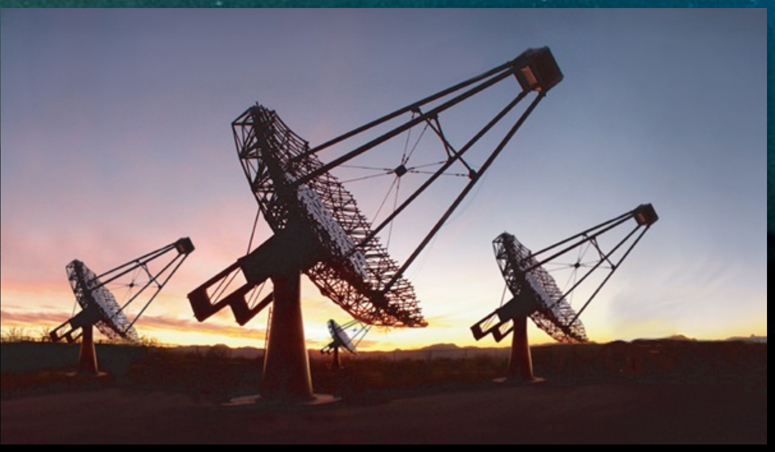

Dark matter halo

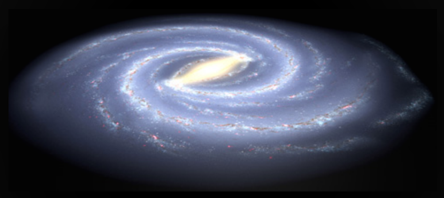

Dark matter in the galaxy

Dwarf spheroidal galaxies

Milky Way **dwarf spheroidal galaxies (dSphs)** are ideal candidates for indirect DM searches, due to their high DM-luminous mass ratios and relative proximity.

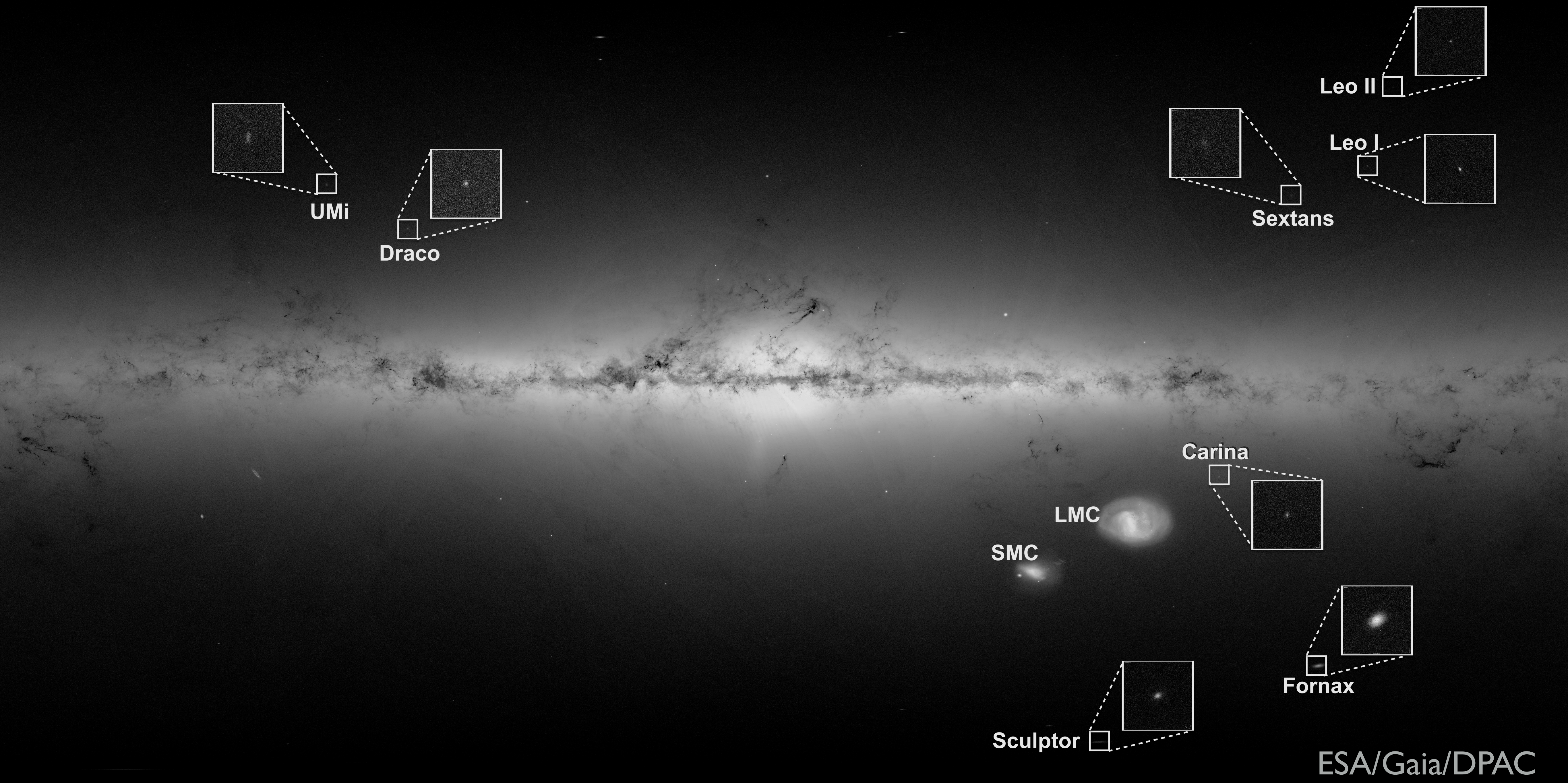

Dwarf spheroidal galaxies

Milky Way **dwarf spheroidal galaxies (dSphs)** are ideal candidates for indirect DM searches, due to their high DM-luminous mass ratios and relative proximity.

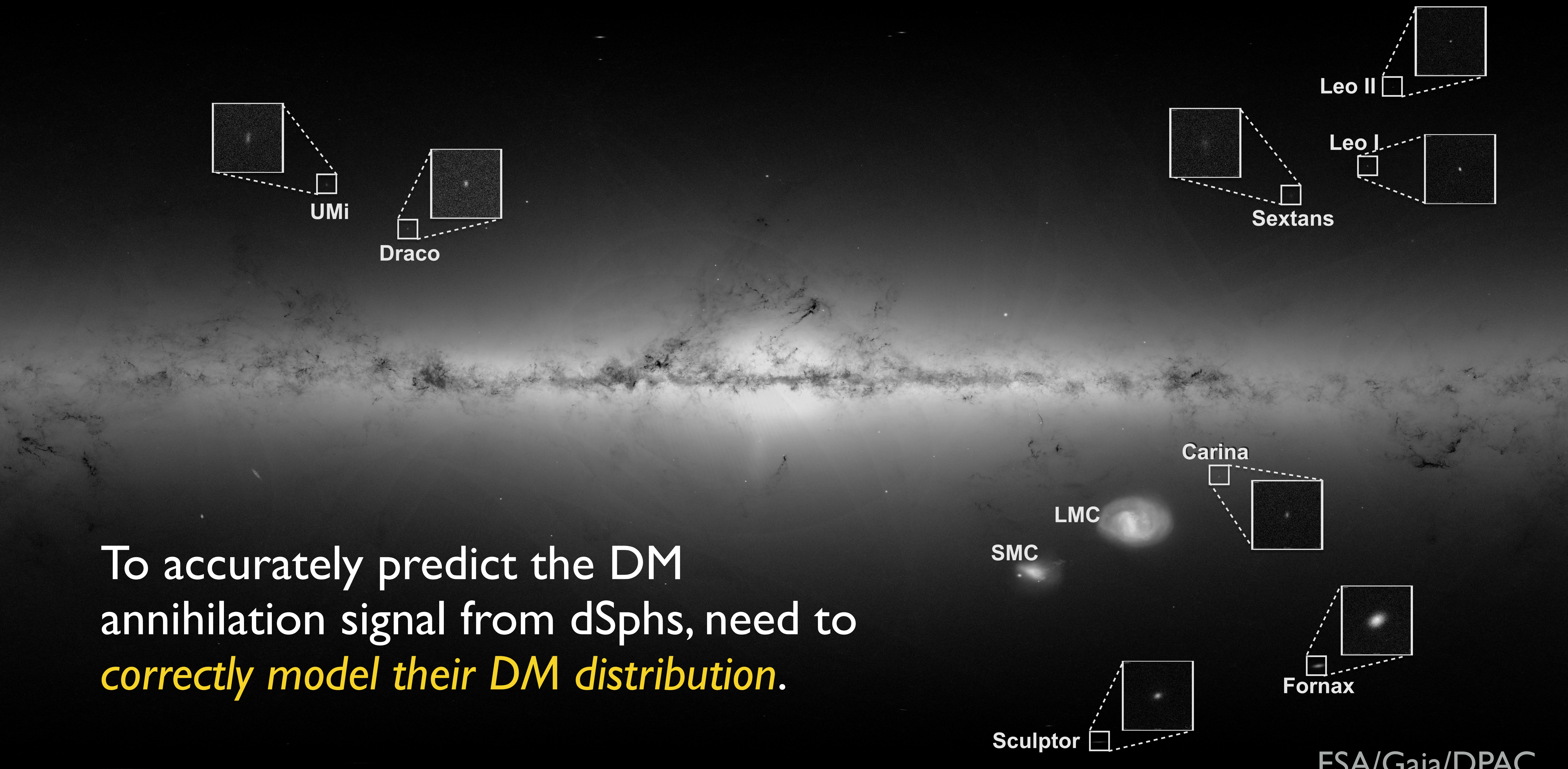

To accurately predict the DM annihilation signal from dSphs, need to *correctly model their DM distribution*.

ESA/Gaia/DPAC

Dark matter distribution in dSphs

Use **high resolution cosmological simulations** to extract the DM distribution in dSphs.

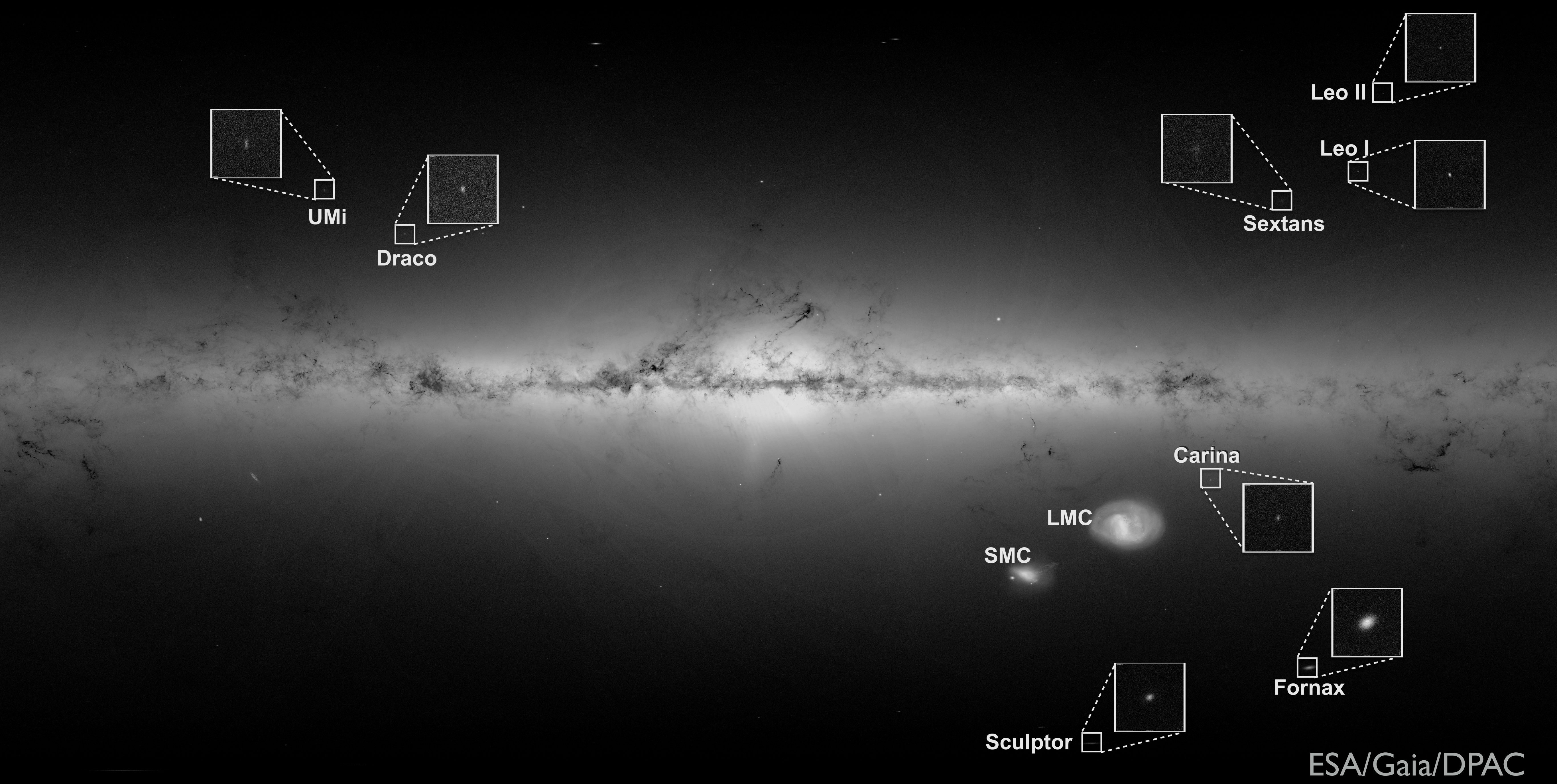

Dark matter distribution in dSphs

Use **high resolution cosmological simulations** to extract the DM distribution in dSphs.

*1. What is the impact of DM distribution modeling on annihilation signals in **Milky Way dSphs**?*

Blanchette et al., JCAP 03, 021 (2023)

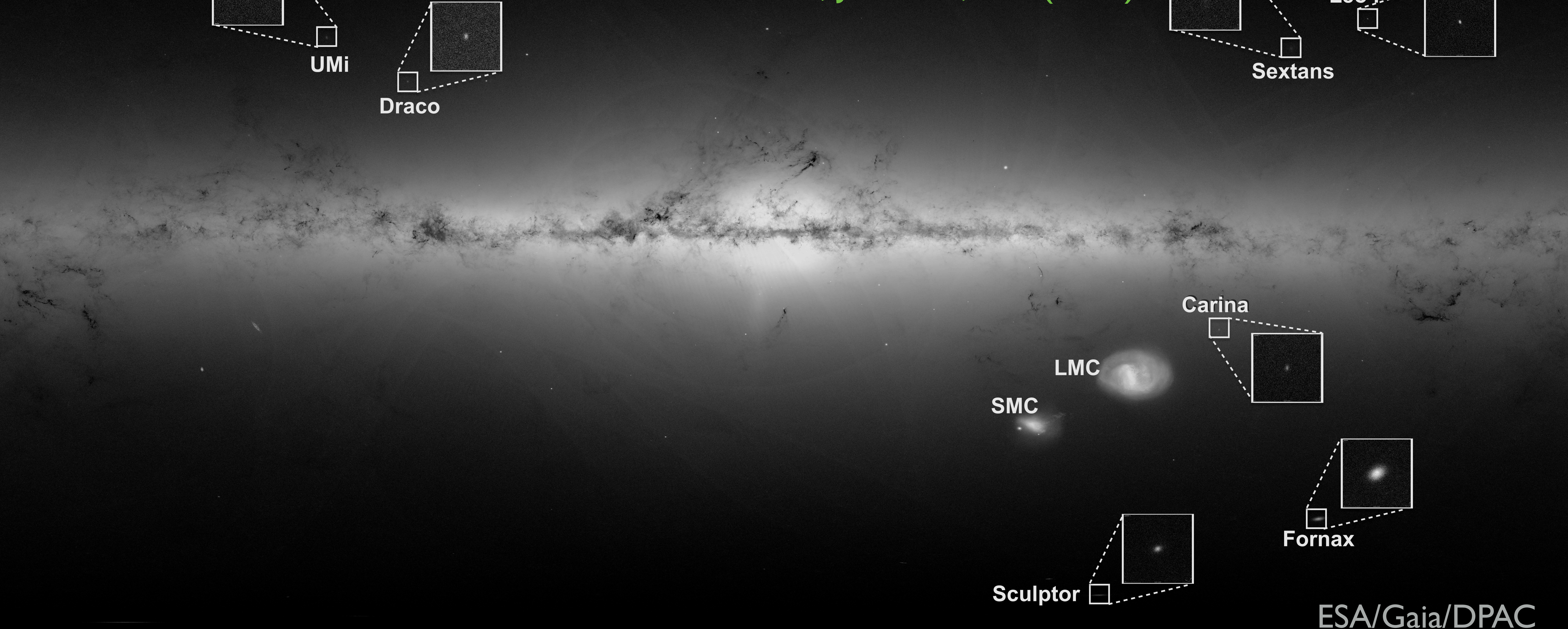

ESA/Gaia/DPAC

Dark matter distribution in dSphs

Use **high resolution cosmological simulations** to extract the DM distribution in dSphs.

*1. What is the impact of DM distribution modeling on annihilation signals in **Milky Way dSphs**?*

Blanchette et al., JCAP 03, 021 (2023)

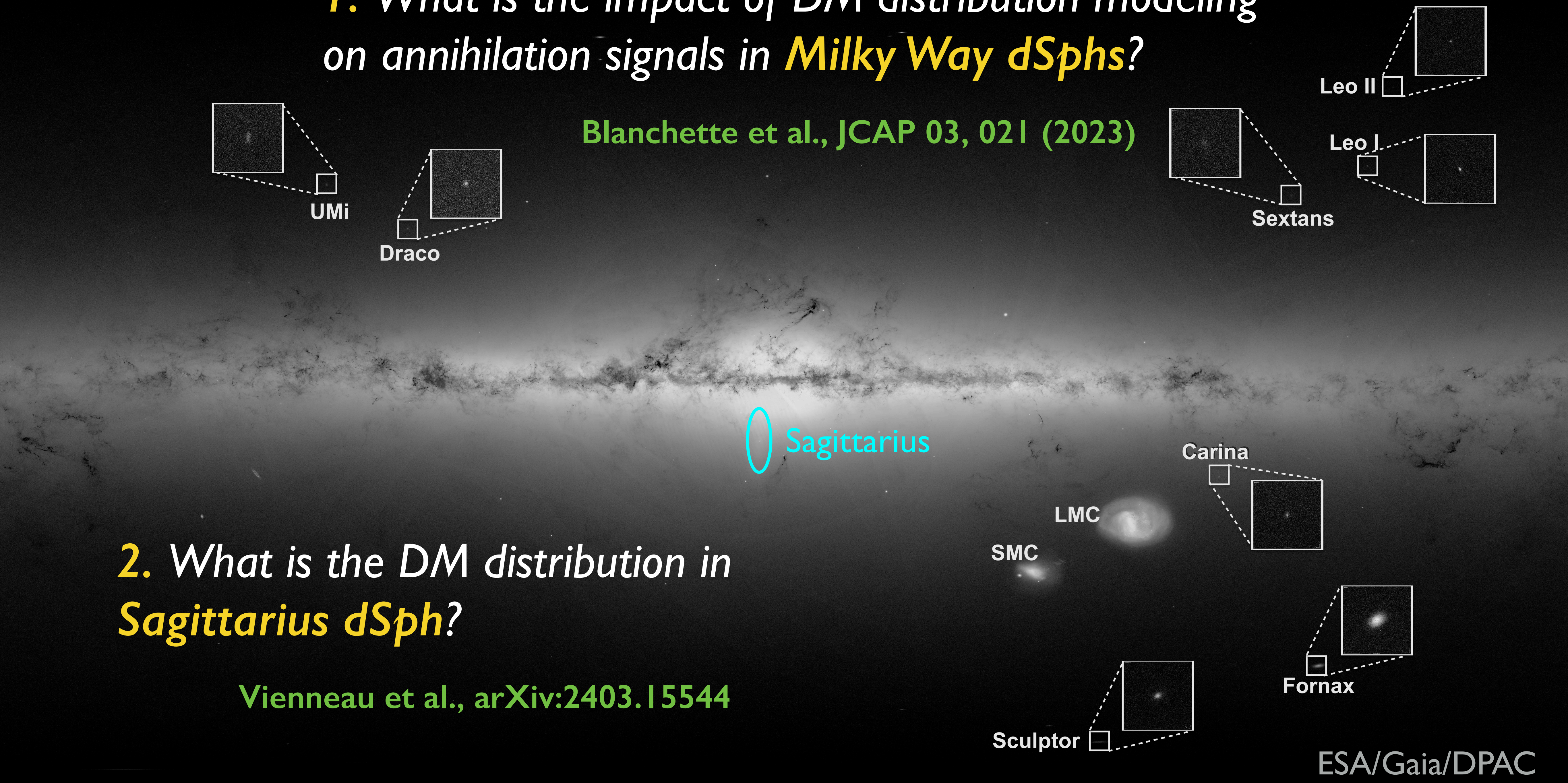

*2. What is the DM distribution in **Sagittarius dSph**?*

Vienneau et al., arXiv:2403.15544

Velocity-independent annihilation

- For the standard **s-wave annihilation**, the DM annihilation cross section is *velocity-independent*, and the expected gamma-ray flux from DM annihilation is:

$$\frac{d\Phi_\gamma}{dE} = \frac{\langle \sigma_A v_{\rm rel} \rangle}{8\pi m_\chi^2} \frac{dN_\gamma}{dE} \int_{\rm l.o.s} d\ell \left[\rho\left(r\left(\ell,\theta\right)\right)\right]^2$$

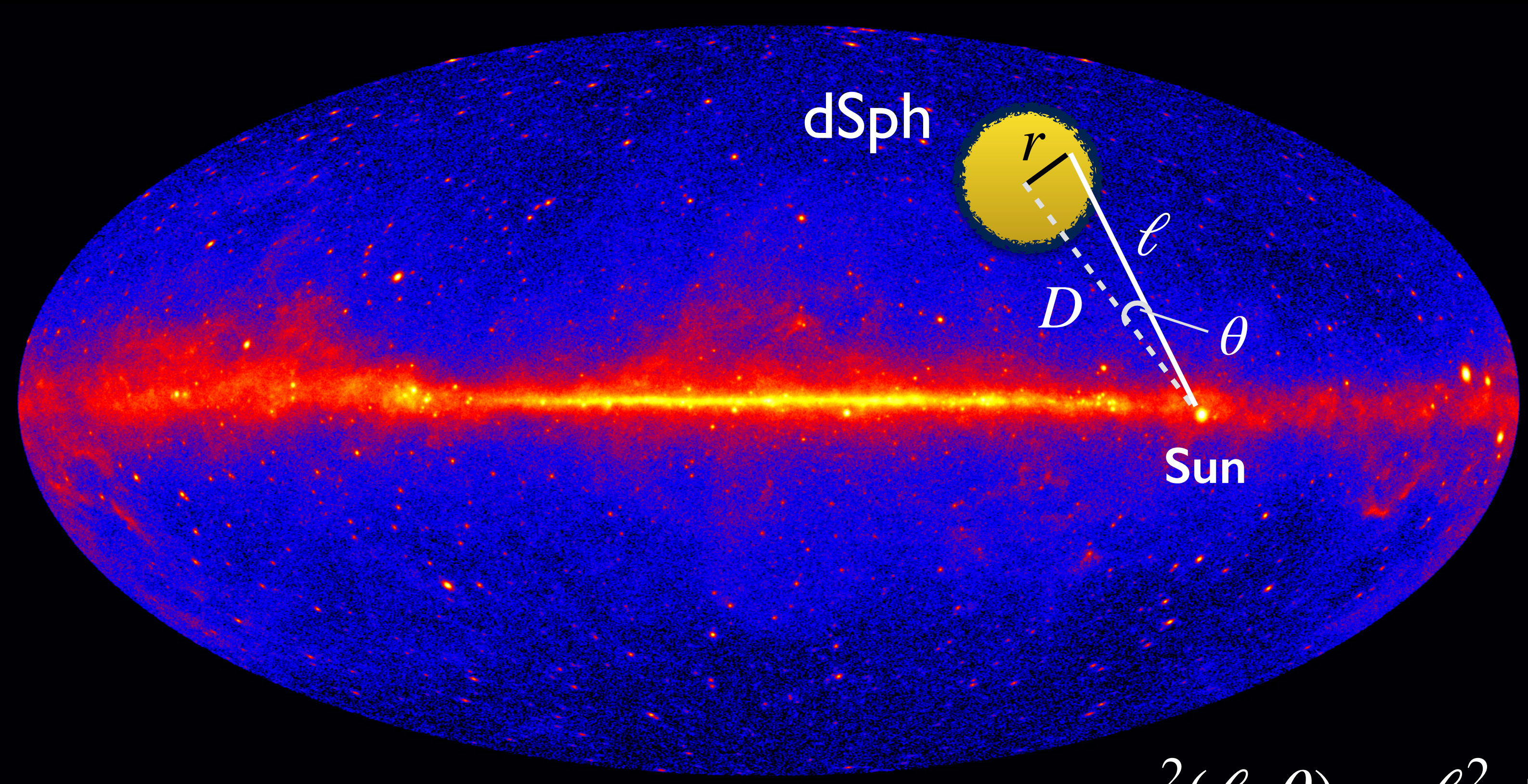

$$r^2(\ell,\theta) = \ell^2 + D^2 - 2\ell D \cos\theta$$

Velocity-independent annihilation

- For the standard **s-wave annihilation**, the DM annihilation cross section is *velocity-independent*, and the expected gamma-ray flux from DM annihilation is:

$\mathcal{J}$-factor

astrophysics

$$\frac{d\Phi_\gamma}{dE} = \frac{\langle \sigma_A v_{\rm rel} \rangle}{8\pi m_\chi^2} \frac{dN_\gamma}{dE} \int_{\rm l.o.s} d\ell \left[\rho\left(r\left(\ell,\theta\right)\right)\right]^2$$

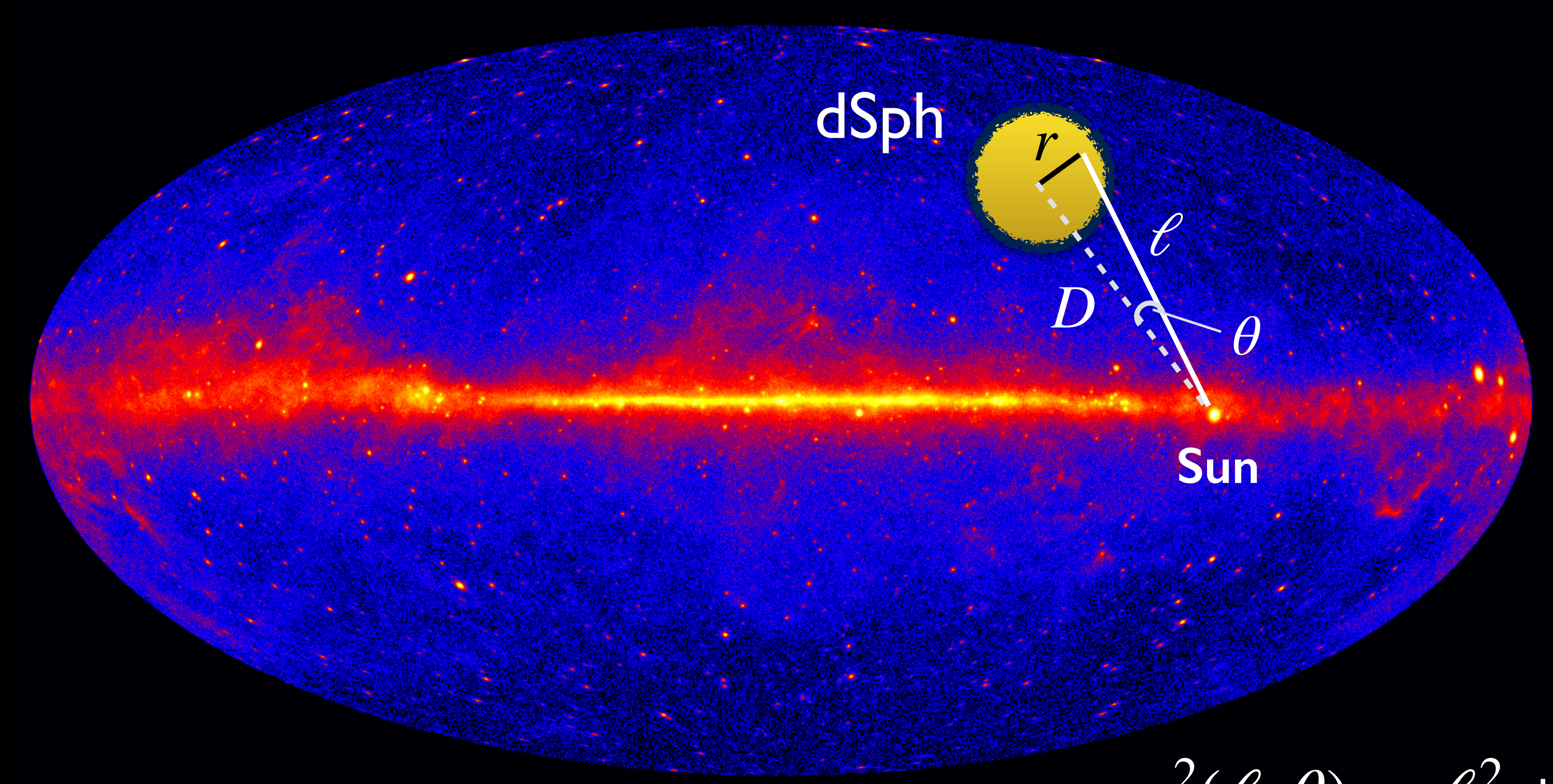

$$r^2(\ell,\theta) = \ell^2 + D^2 - 2\ell D \cos\theta$$

Velocity-dependent annihilation

- For *velocity-dependent* models, the J-factor must also include the DM pair-wise relative velocity distribution.

Velocity-dependent annihilation

- For *velocity-dependent* models, the J-factor must also include the DM pair-wise relative velocity distribution.

- The annihilation cross section averaged over the relative velocity distribution is defined as:

$$\langle \sigma_A v_{\rm rel} \rangle (\mathbf{x}) = \int d^3 \mathbf{v}_{\rm rel} \, P_{\mathbf{x}}(\mathbf{v}_{\rm rel}) \, (\sigma_A v_{\rm rel})$$

DM relative velocity distribution at position $\mathbf{x}$ in the subhalo

Velocity-dependent annihilation

- For *velocity-dependent* models, the J-factor must also include the DM pair-wise relative velocity distribution.

- The annihilation cross section averaged over the relative velocity distribution is defined as:

$$\langle \sigma_A v_{\rm rel} \rangle(\mathbf{x}) = \int d^3\mathbf{v}_{\rm rel}\, P_{\mathbf{x}}(\mathbf{v}_{\rm rel})\, (\sigma_A v_{\rm rel})$$

$P_{\mathbf{x}}$ ↓ DM relative velocity distribution at position $\mathbf{x}$ in the subhalo

- Parametrize $\sigma_A v_{\rm rel}$ in the general form:

$$\sigma_A v_{\rm rel} = (\sigma_A v_{\rm rel})_0\, (v_{\rm rel}/c)^n$$

$(\sigma_A v_{\rm rel})_0$ ↙ velocity-independent component of the cross section

Velocity-dependent annihilation

- For *velocity-dependent* models, the J-factor must also include the DM pair-wise relative velocity distribution.

- The annihilation cross section averaged over the relative velocity distribution is defined as:

$$\langle \sigma_A v_{\rm rel} \rangle(\mathbf{x}) = \int d^3\mathbf{v}_{\rm rel}\, P_{\mathbf{x}}(\mathbf{v}_{\rm rel})\, (\sigma_A v_{\rm rel})$$

↓ DM relative velocity distribution at position $\mathbf{x}$ in the subhalo

- Parametrize $\sigma_A v_{\rm rel}$ in the general form:

$$\sigma_A v_{\rm rel} = (\sigma_A v_{\rm rel})_0\, (v_{\rm rel}/c)^n$$

↙ velocity-independent component of the cross section

Different annihilation models:

- $n = 0$: **s-wave**
- $n = 2$: **p-wave**
- $n = 4$: **d-wave**
- $n = -1$: **Sommerfeld**

Velocity-dependent annihilation

- The expected gamma-ray flux from DM annihilation:

$$\frac{d\Phi_\gamma}{dE} = \frac{(\sigma_A v_{\rm rel})_0}{8\pi m_\chi^2}\frac{dN_\gamma}{dE}\mathcal{J}_s$$

written in terms of the **effective J-factor**:

$$\mathcal{J}_s(\theta) = \int d\ell \, \frac{\langle \sigma_A v_{\rm rel}\rangle}{(\sigma_A v_{\rm rel})_0}\left[\rho\left(r\left(\ell,\theta\right)\right)\right]^2$$

Velocity-dependent annihilation

- The expected gamma-ray flux from DM annihilation:

$$\frac{d\Phi_\gamma}{dE} = \frac{(\sigma_A v_{\rm rel})_0}{8\pi m_\chi^2}\frac{dN_\gamma}{dE}\mathscr{J}_s$$

written in terms of the **effective J-factor**:

$$\mathscr{J}_s(\theta) = \int d\ell \, \frac{\langle \sigma_A v_{\rm rel}\rangle}{(\sigma_A v_{\rm rel})_0}\left[\rho\left(r\left(\ell,\theta\right)\right)\right]^2$$

$$= \int d\ell \int d^3\mathbf{v}_{\rm rel}\, P_{\mathbf{x}}(\mathbf{v}_{\rm rel})\left(\frac{v_{\rm rel}}{c}\right)^n \left[\rho\left(r\left(\ell,\theta\right)\right)\right]^2$$

Velocity-dependent annihilation

- The expected gamma-ray flux from DM annihilation:

$$\frac{d\Phi_\gamma}{dE} = \frac{(\sigma_A v_{\rm rel})_0}{8\pi m_\chi^2} \frac{dN_\gamma}{dE} \mathcal{J}_s$$

written in terms of the **effective J-factor**:

$$\mathcal{J}_s(\theta) = \int d\ell \, \frac{\langle \sigma_A v_{\rm rel} \rangle}{(\sigma_A v_{\rm rel})_0} \left[\rho\left(r\left(\ell,\theta\right)\right)\right]^2$$

$$= \int d\ell \int d^3\mathbf{v}_{\rm rel}\, P_{\mathbf{x}}(\mathbf{v}_{\rm rel}) \left(\frac{v_{\rm rel}}{c}\right)^n \left[\rho\left(r\left(\ell,\theta\right)\right)\right]^2$$

- The J-factor integrated over solid angle:

$$\widetilde{\mathcal{J}}_s(\theta) = 2\pi \int_0^\theta \mathcal{J}_s(\theta') \sin\theta' d\theta'$$

Velocity-dependent annihilation

- The **effective J-factor**:

$$\mathcal{J}_s(\theta) = \int d\ell \int d^3\mathbf{v}_{\rm rel}\, P_{\mathbf{x}}(\mathbf{v}_{\rm rel}) \left(\frac{v_{\rm rel}}{c}\right)^n \left[\rho\left(r\left(\ell,\theta\right)\right)\right]^2$$

- DM particles in dwarfs have low velocity dispersion. → DM annihilation expected to be *suppressed* for p-wave ($n = 2$) and d-wave ($n = 4$), and *enhanced* for Sommerfeld ($n = -1$) models.

Dark matter distribution in dSphs

Use **high resolution cosmological simulations** to extract the DM distribution in dSphs.

*1. What is the impact of DM distribution modeling on annihilation signals in **Milky Way dSphs**?*

Blanchette et al., JCAP 03, 021 (2023)

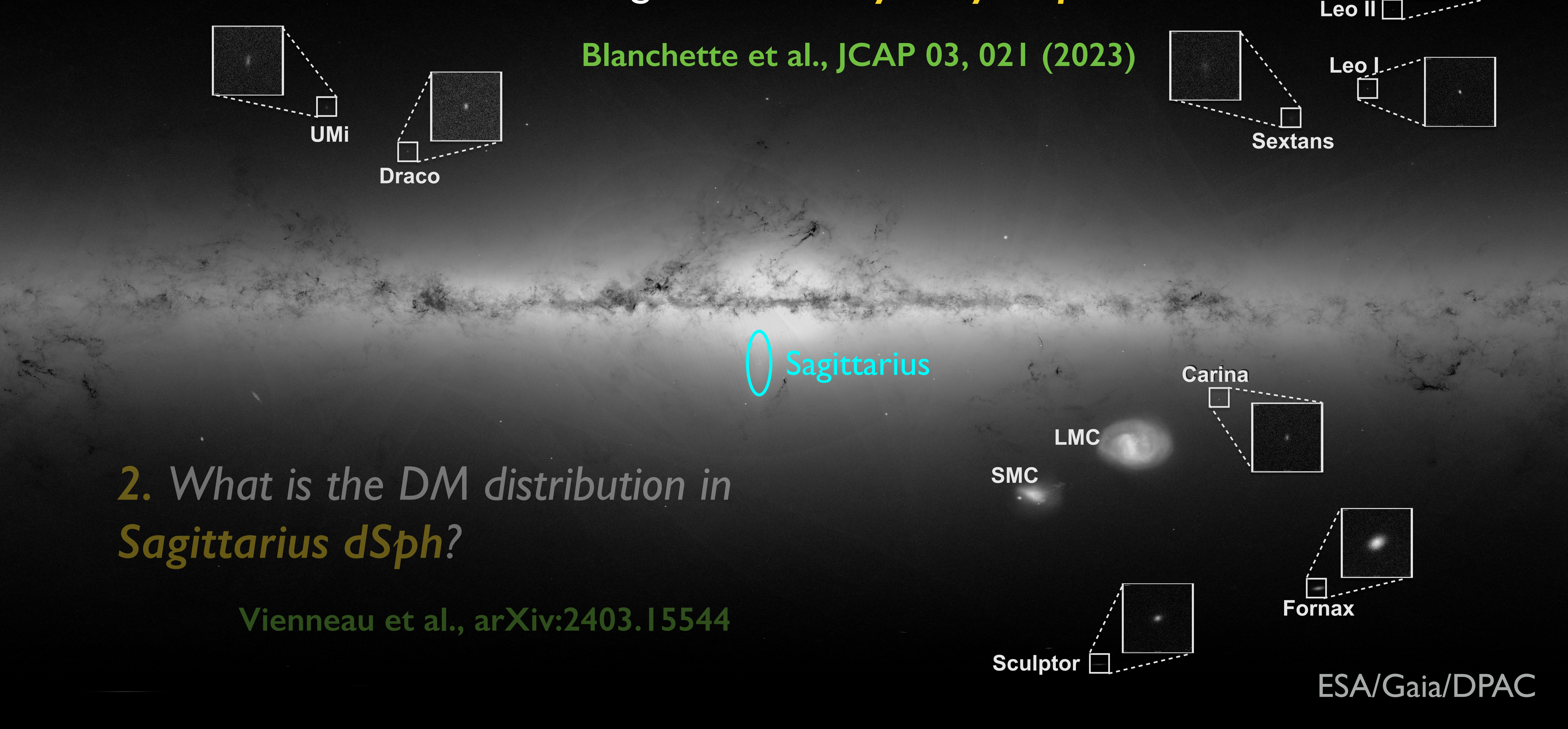

*2. What is the DM distribution in **Sagittarius dSph**?*

Vienneau et al., arXiv:2403.15544

APOSTLE simulations

Zoomed simulations of Local Group analogue systems containing two Milky Way mass systems.

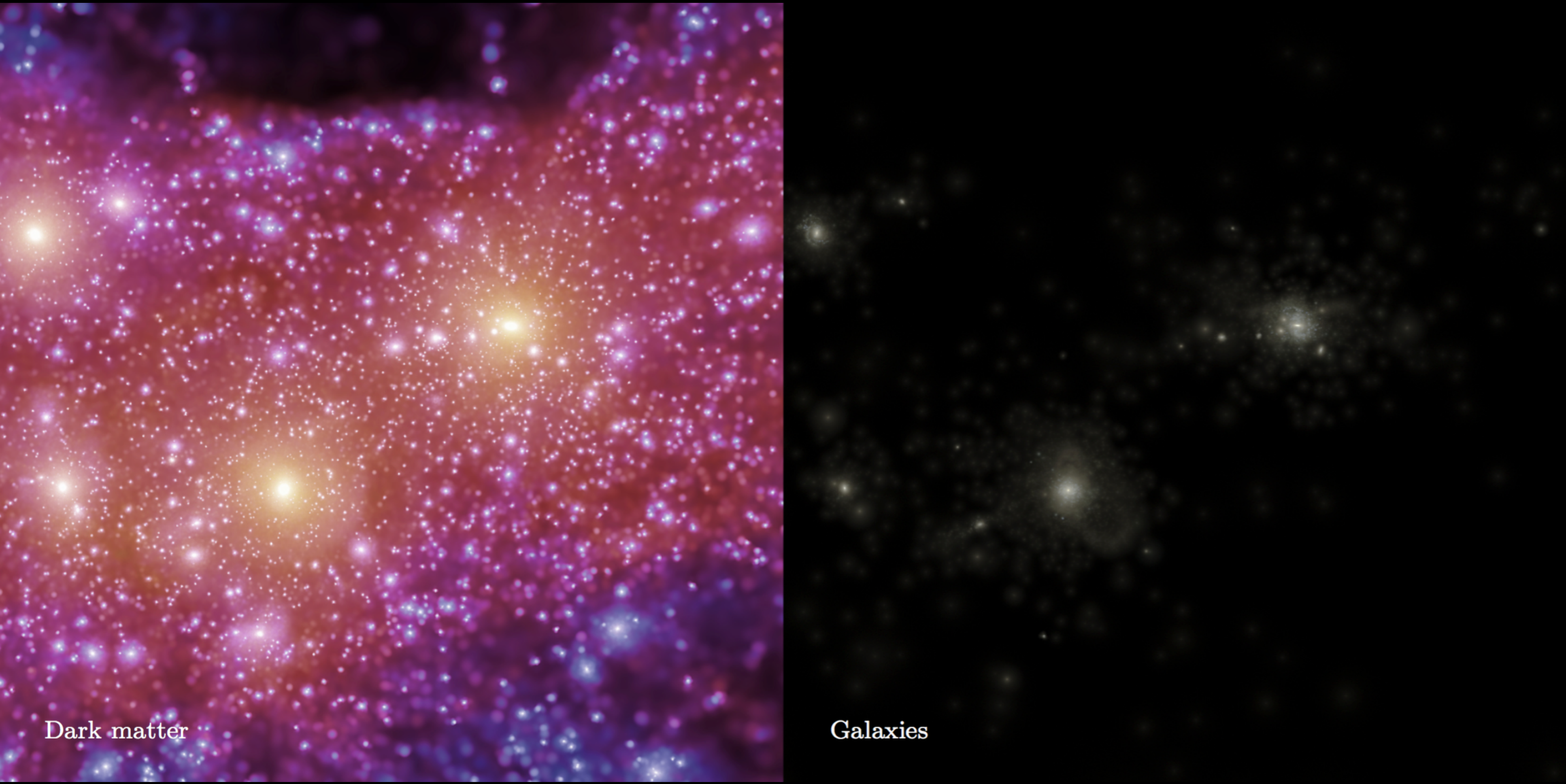

APOSTLE simulations

Zoomed simulations of Local Group analogue systems containing two Milky Way mass systems.

Study 10 Milky Way-like halos simulated at the highest resolution available:

m_{DM} [$M_\odot$]	m_b [$M_\odot$]	ϵ [pc]
5×10^4	10^4	134

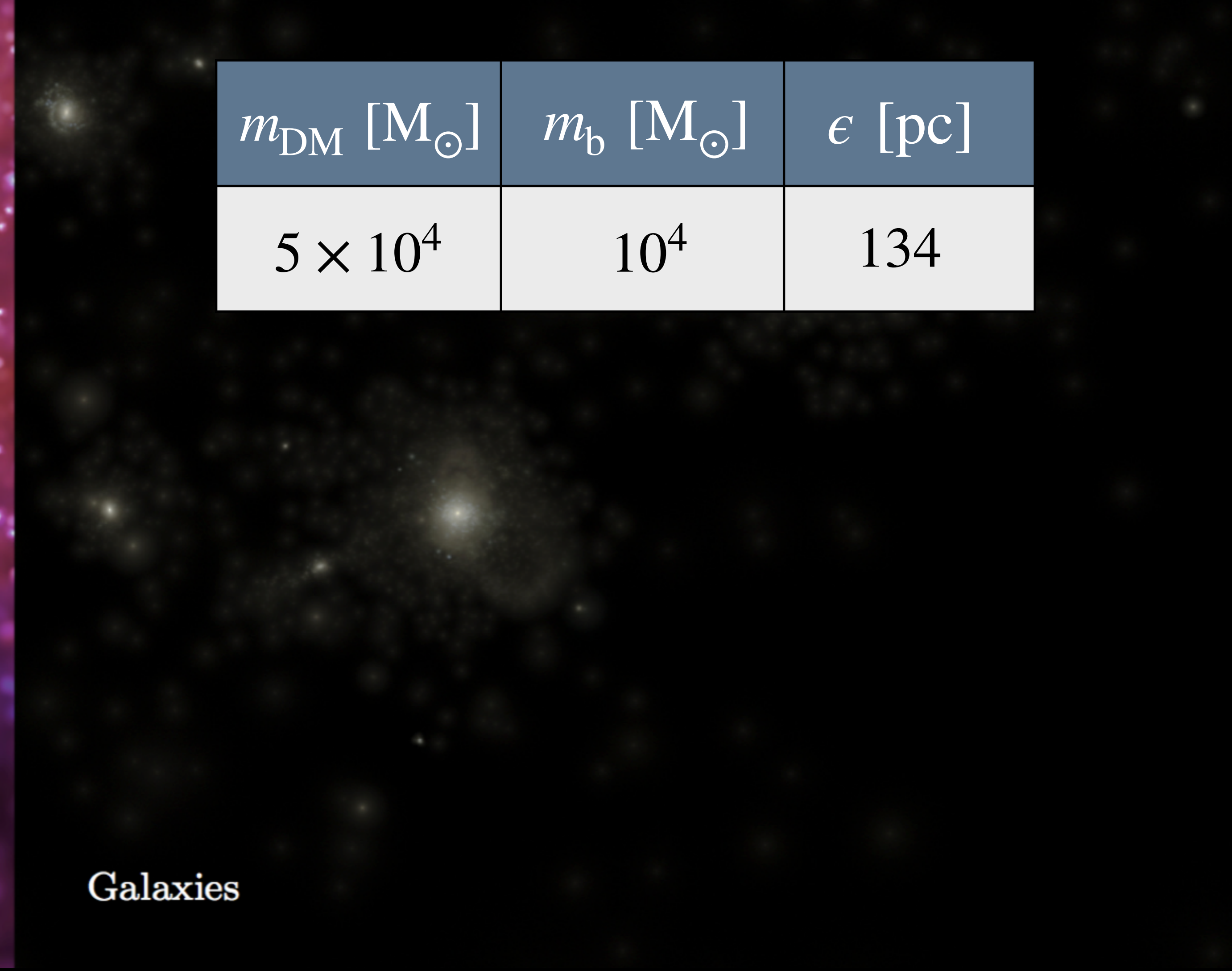

APOSTLE simulations

Zoomed simulations of Local Group analogue systems containing two Milky Way mass systems.

Study 10 Milky Way-like halos simulated at the highest resolution available:

$m_{\rm DM}$ [$M_\odot$]	$m_{\rm b}$ [$M_\odot$]	ϵ [pc]
5×10^4	10^4	134

These halos include 2074 subhalos that have nonzero stellar mass and a total mass of $\approx [10^7 - 10^{10}]\ M_\odot$

Galaxies

Selection of dSph analogues

- Identify dSph analogues by matching to observed properties: **stellar mass** and **circular velocity at half-light radius**.

dSph Analogue	N	$M_\star^{\rm obs}$ [$M_\odot$]	$M_\star$ [$M_\odot$]	$V_{1/2}^{\rm obs}$ [km/s]	$V_{1/2}$ [km/s]
Canes Venatici I (1)	21	2.3×10^5	5.66×10^5	13.2	14.56
Canes Venatici I (2)			2.50×10^5		14.79
Carina (1)	17	4.3×10^5	2.38×10^5	11.1	11.30
Carina (2)			9.30×10^5		11.37
Draco (1)	4	2.2×10^5	8.91×10^5	17.5	14.92
Draco (2)			8.89×10^5		15.28
Fornax (1)	4	1.7×10^7	1.36×10^7	18.5	18.79
Fornax (2)			1.20×10^7		18.36
Leo I (1)	19	5.0×10^6	3.27×10^6	15.6	15.24
Leo I (2)			3.52×10^6		15.15
Leo II (1)	47	7.8×10^5	1.45×10^6	11.4	12.15
Leo II (2)			6.86×10^5		10.58
Sculptor (1)	9	2.5×10^6	1.40×10^6	15.6	14.97
Sculptor (2)			5.52×10^6		15.81
Sextans (1)	3	5.9×10^5	3.89×10^5	12.3	12.77
Sextans (2)			3.88×10^6		11.61
Ursa Minor (1)	23	3.9×10^5	4.61×10^5	19.9	19.13
Ursa Minor (2)			8.91×10^5		19.28

Selection of dSph analogues

- Identify dSph analogues by matching to observed properties: **stellar mass** and **circular velocity at half-light radius.**
  → 100 unique dSph analogues

dSph Analogue	N	$M_\star^{obs}$ [$M_\odot$]	$M_\star$ [$M_\odot$]	$V_{1/2}^{obs}$ [km/s]	$V_{1/2}$ [km/s]
Canes Venatici I (1)	21	2.3×10^5	5.66×10^5	13.2	14.56
Canes Venatici I (2)			2.50×10^5		14.79
Carina (1)	17	4.3×10^5	2.38×10^5	11.1	11.30
Carina (2)			9.30×10^5		11.37
Draco (1)	4	2.2×10^5	8.91×10^5	17.5	14.92
Draco (2)			8.89×10^5		15.28
Fornax (1)	4	1.7×10^7	1.36×10^7	18.5	18.79
Fornax (2)			1.20×10^7		18.36
Leo I (1)	19	5.0×10^6	3.27×10^6	15.6	15.24
Leo I (2)			3.52×10^6		15.15
Leo II (1)	47	7.8×10^5	1.45×10^6	11.4	12.15
Leo II (2)			6.86×10^5		10.58
Sculptor (1)	9	2.5×10^6	1.40×10^6	15.6	14.97
Sculptor (2)			5.52×10^6		15.81
Sextans (1)	3	5.9×10^5	3.89×10^5	12.3	12.77
Sextans (2)			3.88×10^6		11.61
Ursa Minor (1)	23	3.9×10^5	4.61×10^5	19.9	19.13
Ursa Minor (2)			8.91×10^5		19.28

Dark matter density profiles

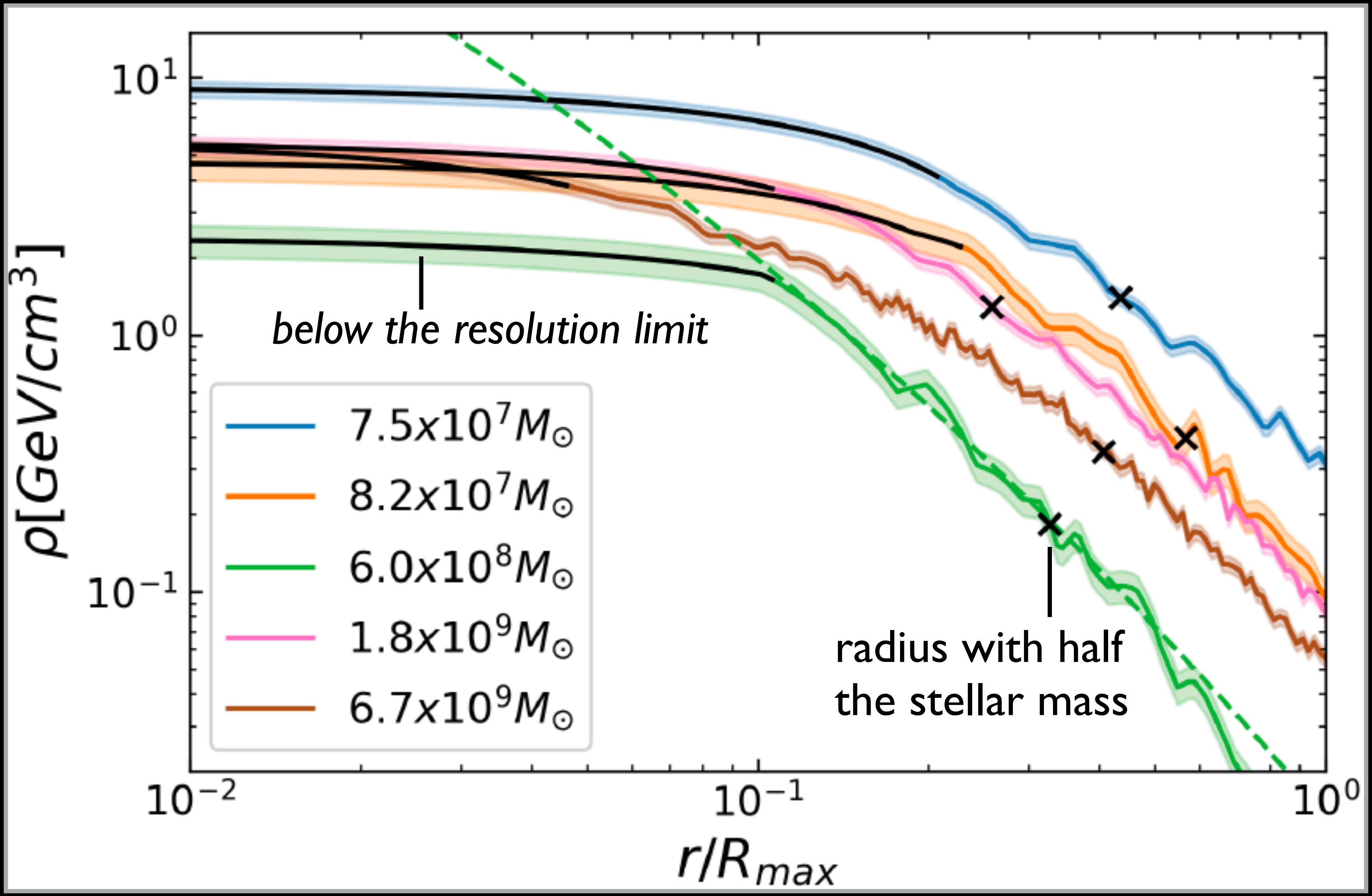

Blanchette et al., JCAP 03, 021 (2023)

Dark matter density profiles

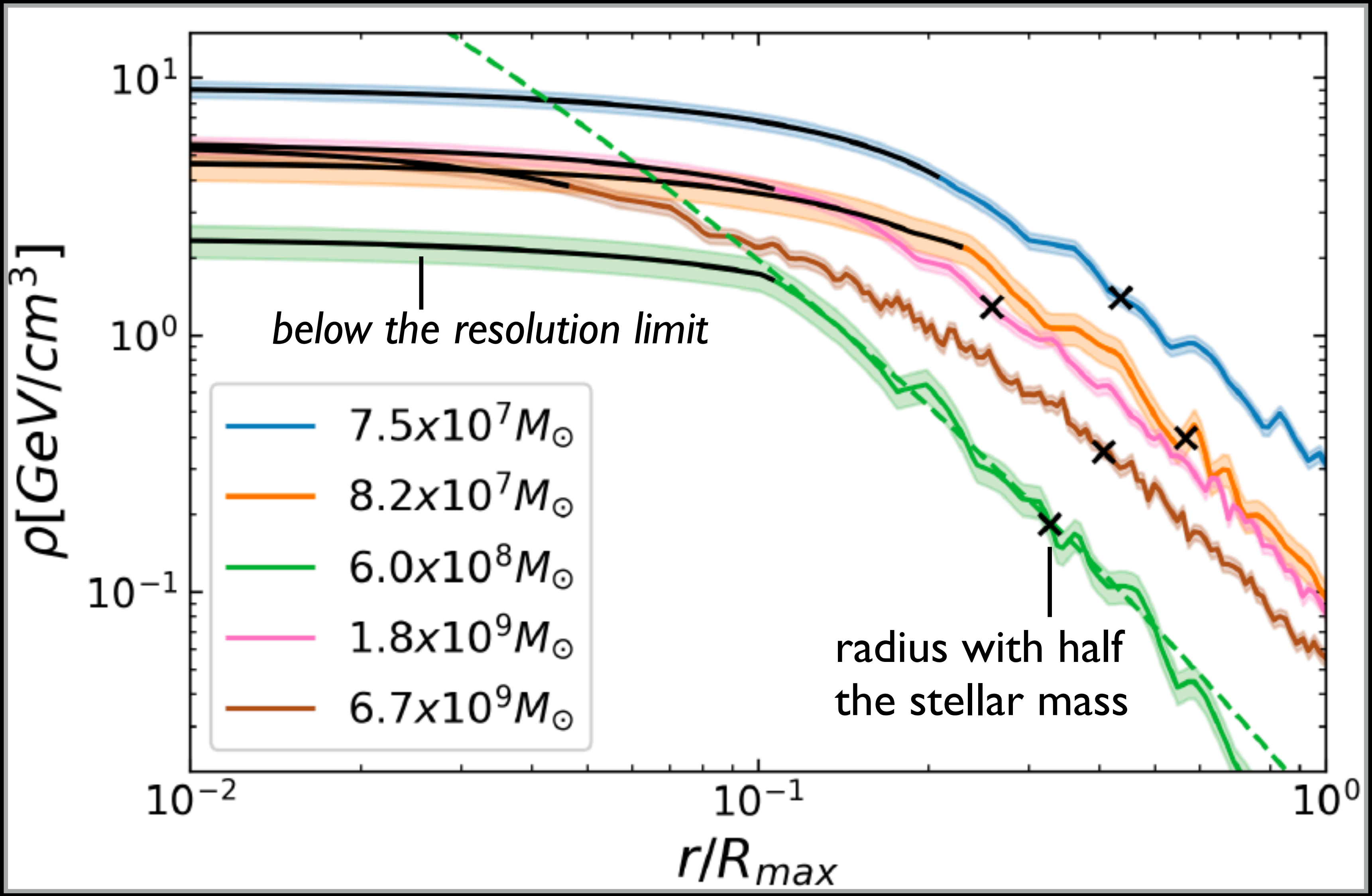

Blanchette et al., JCAP 03, 021 (2023)

- Flattening of the density profiles in the inner regions of the subhalos is due to the resolution limit of the simulations.

Dark matter density profiles

$$\rho = \rho_{-2} \exp\left(-\frac{2}{\alpha}\left[\left(\frac{r}{r_{-2}}\right)^{\alpha} - 1\right]\right)$$

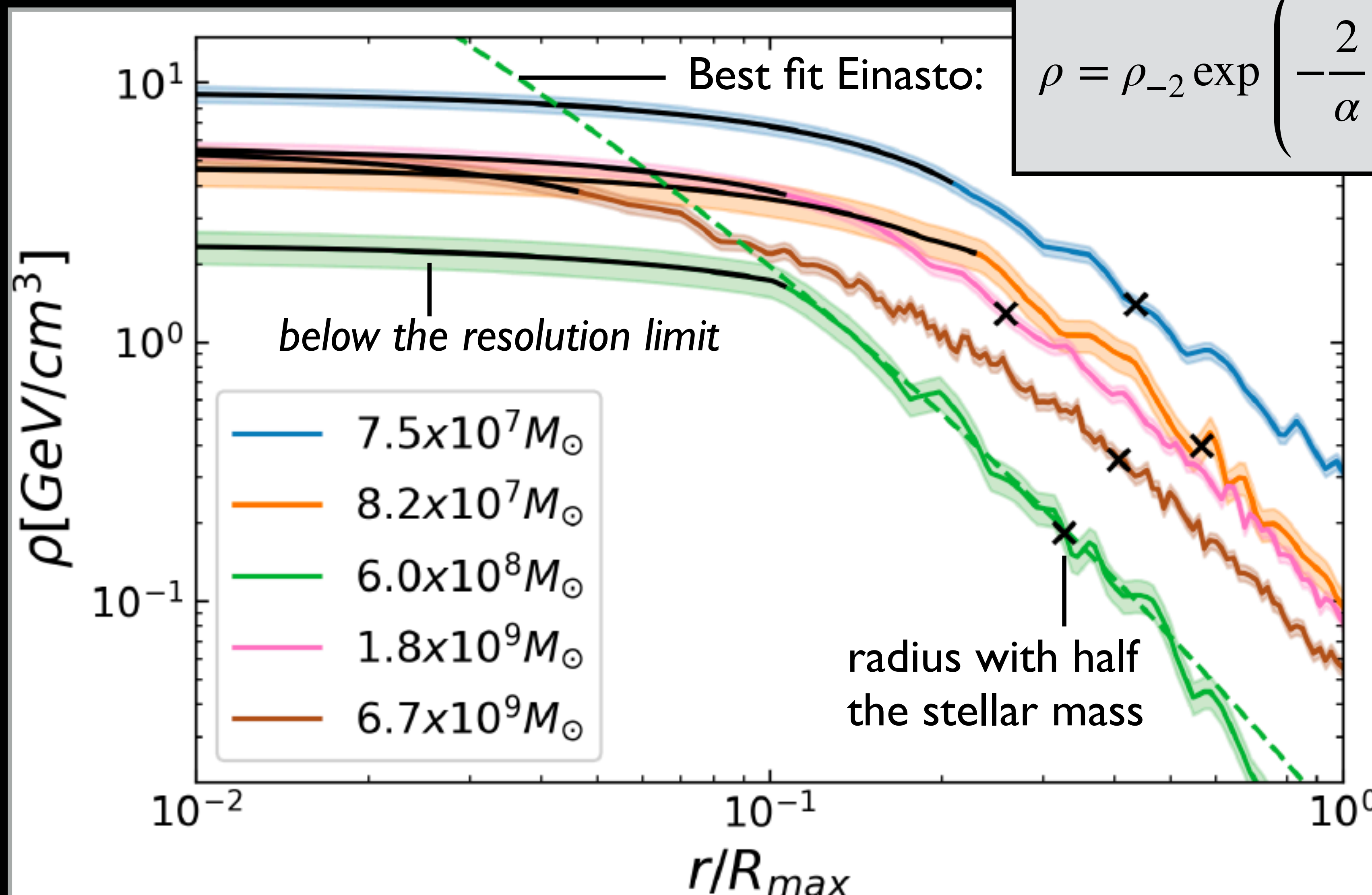

Blanchette et al., JCAP 03, 021 (2023)

- Flattening of the density profiles in the inner regions of the subhalos is due to the resolution limit of the simulations.

DM relative velocity distributions

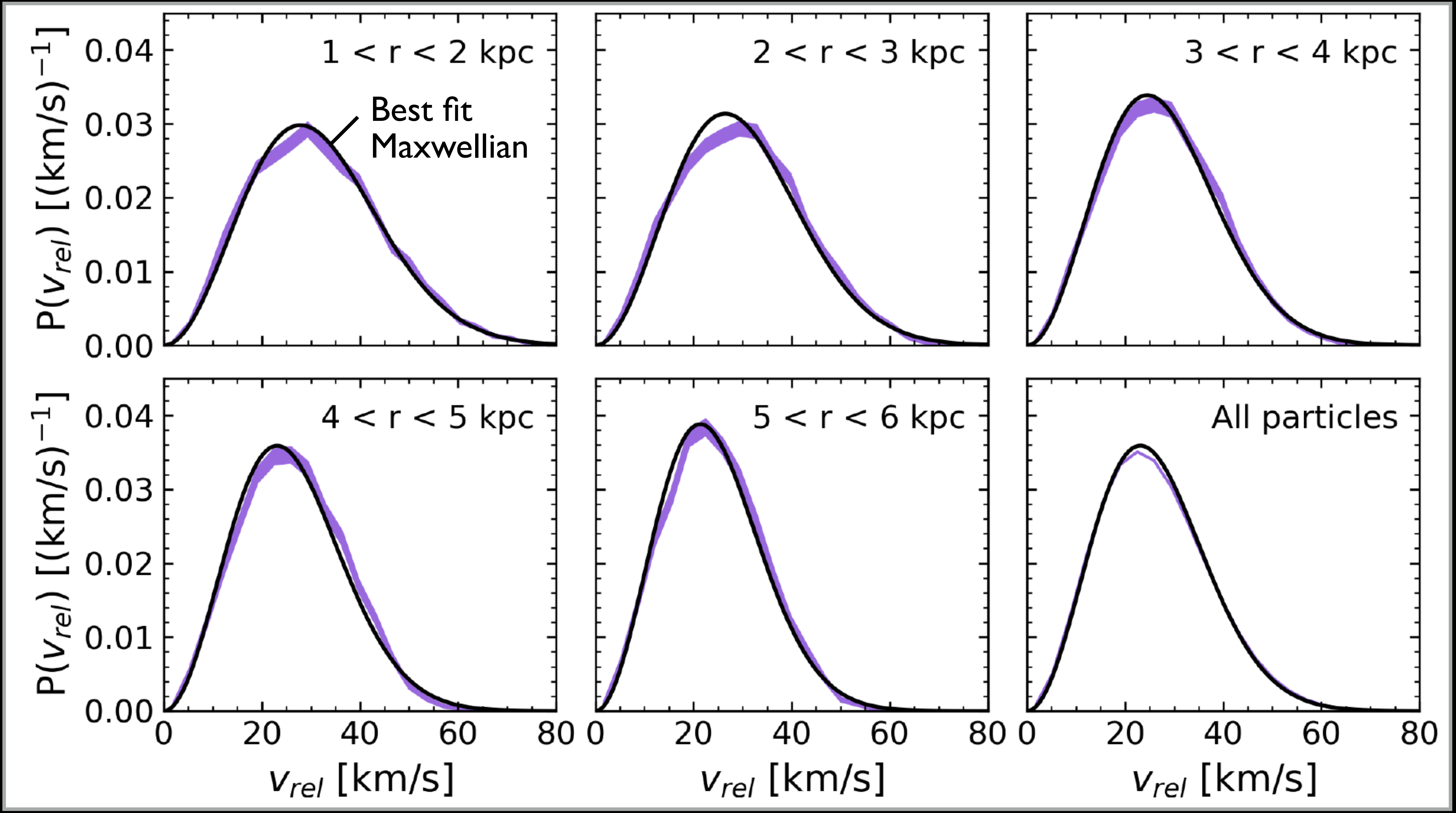

Blanchette et al., JCAP 03, 021 (2023)

- The Maxwellian distribution provides a good fit to the DM relative velocity distribution of the simulated subhalos at all radii.

Power law relation

- Extract a simple power law relation between the peak speed of the Maxwellian distribution and the maximum circular velocity of the dSph analogues.

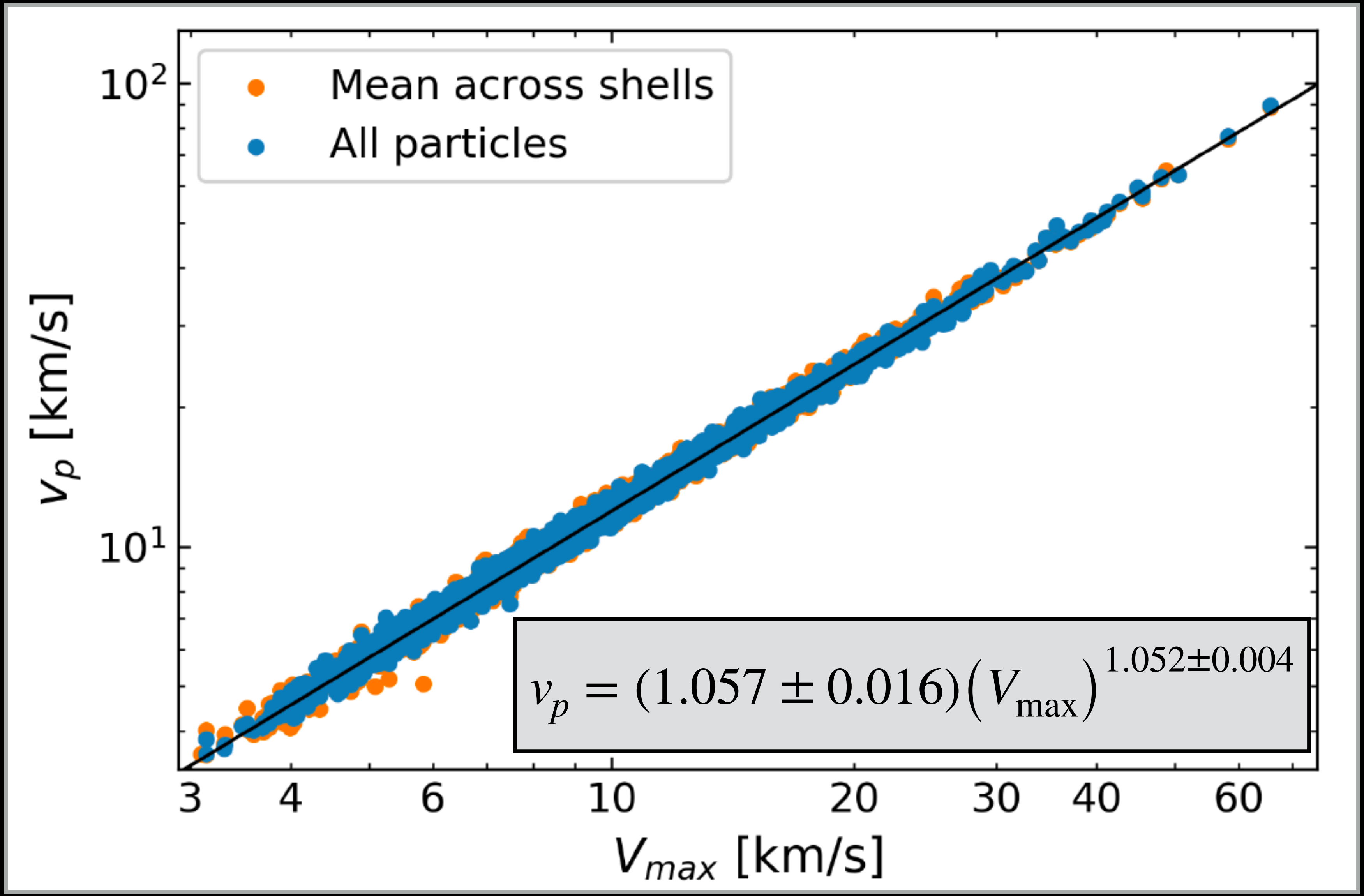

Blanchette et al., JCAP 03, 021 (2023)

Power law relation

- Extract a simple power law relation between the peak speed of the Maxwellian distribution and the maximum circular velocity of the dSph analogues. ➡ *Can be used to accurately model the DM relative velocity distribution.*

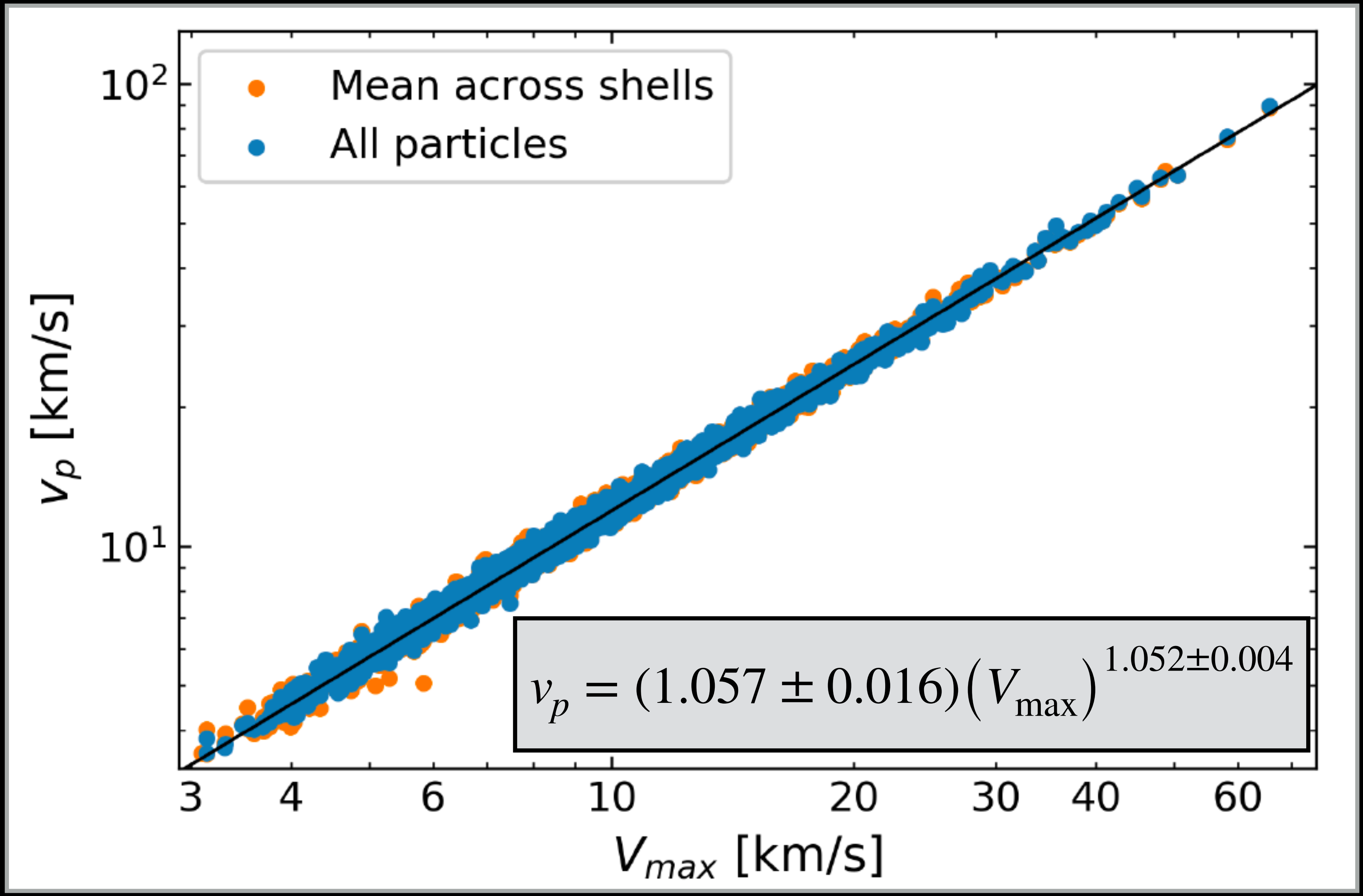

Blanchette et al., JCAP 03, 021 (2023)

Integrated J-factors

Carina analogue

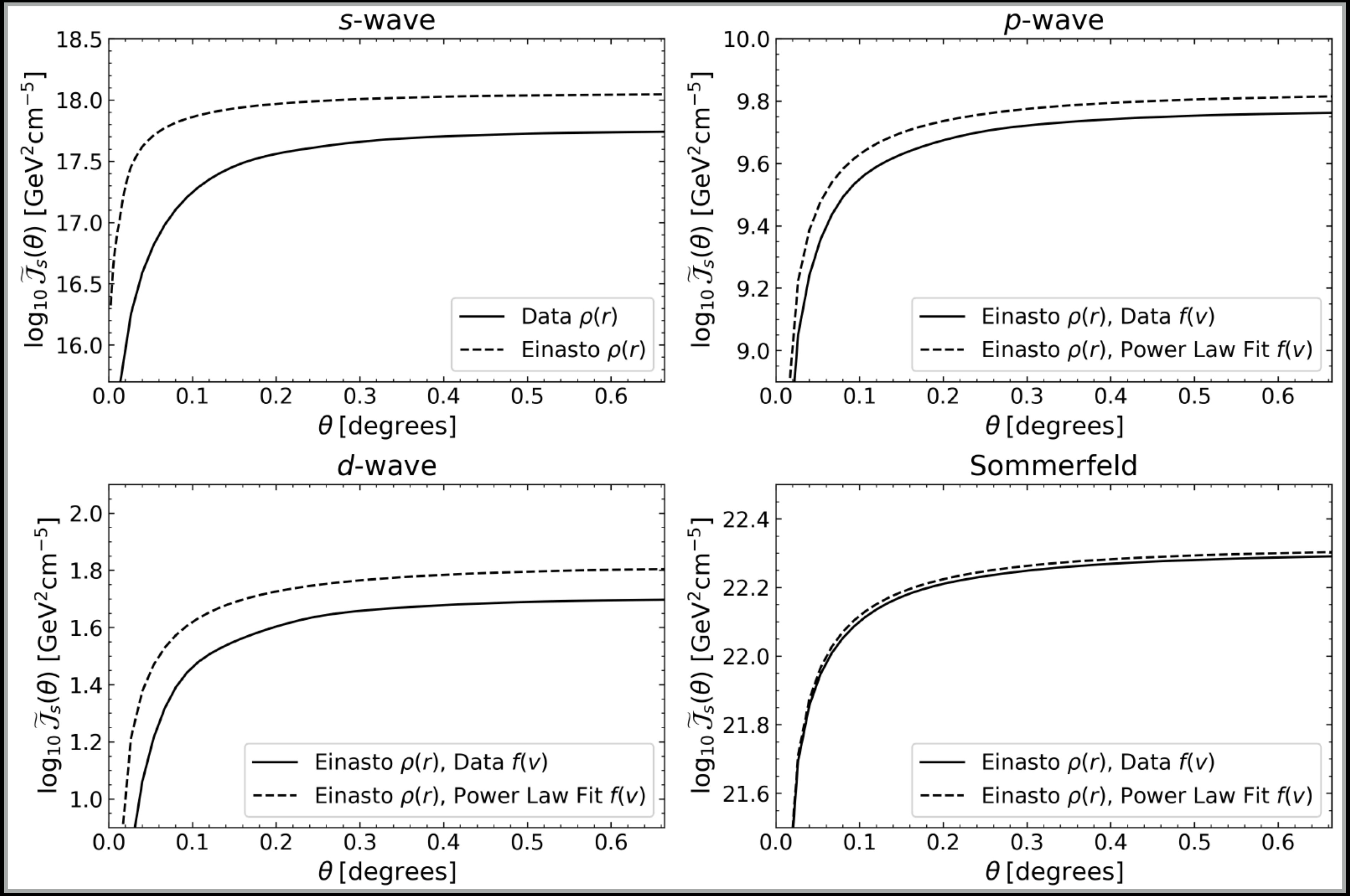

Blanchette et al., JCAP 03, 021 (2023)

Integrated J-factors

Carina analogue

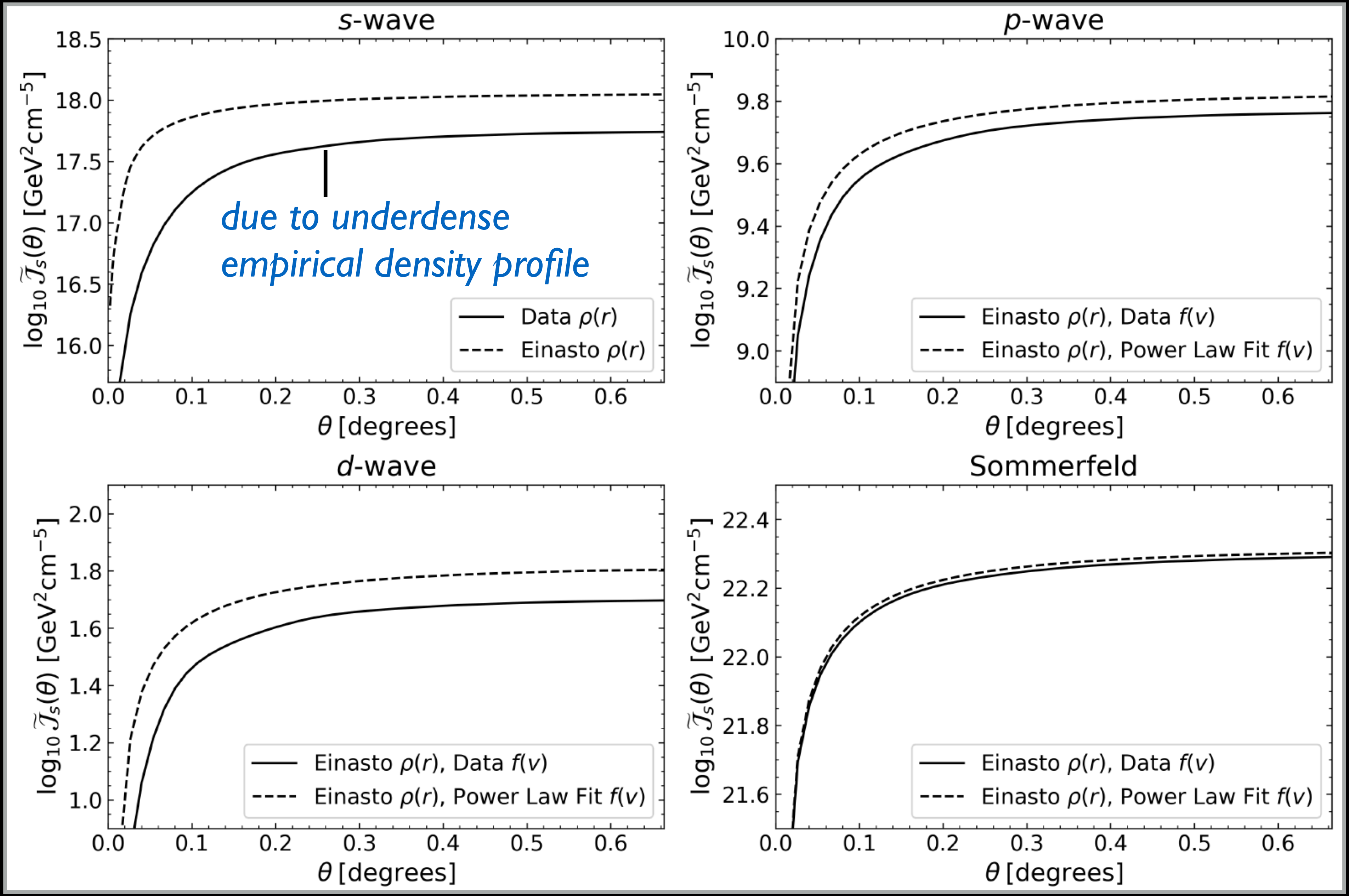

Blanchette et al., JCAP 03, 021 (2023)

Integrated J-factors

Carina analogue

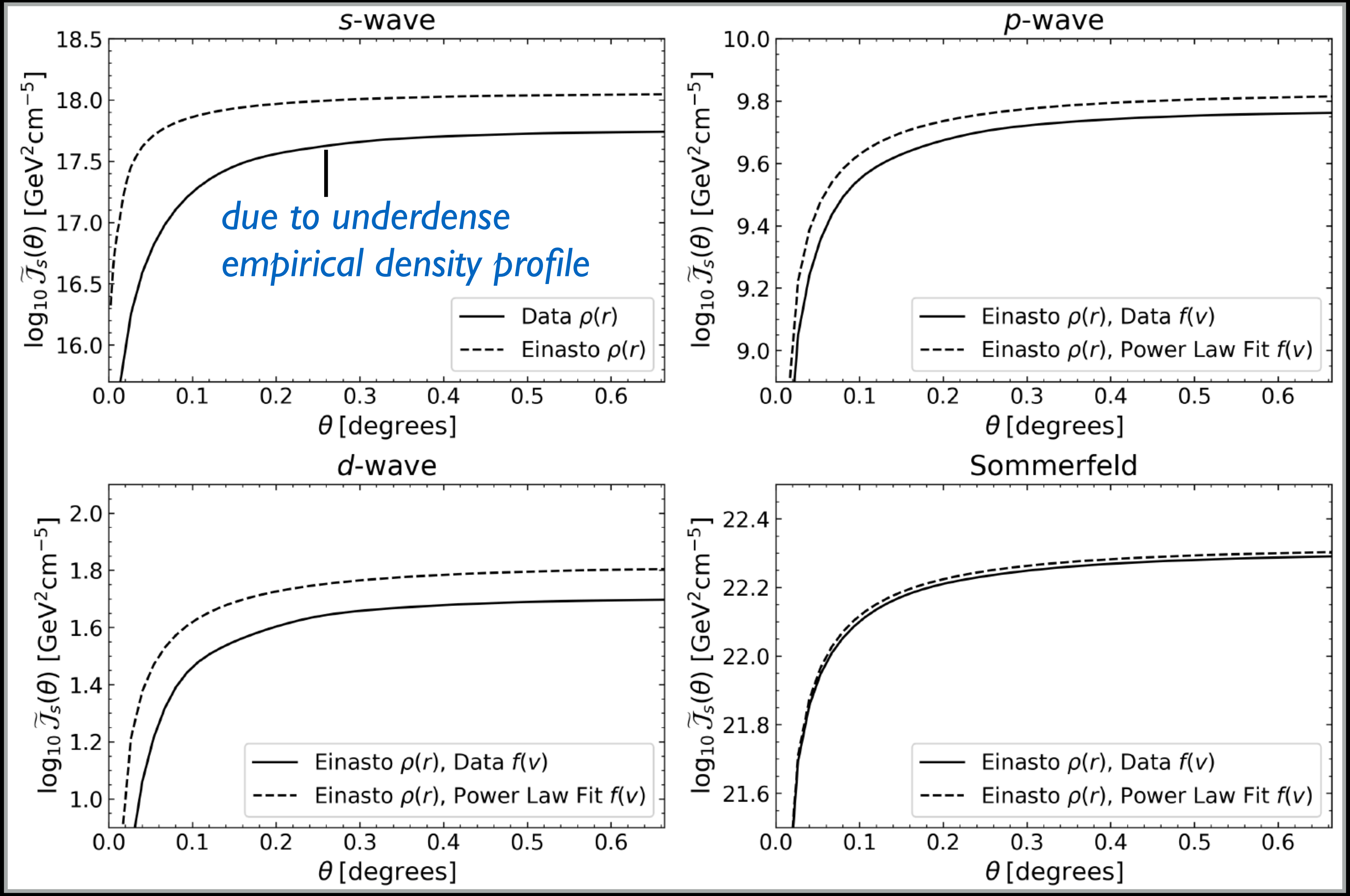

Blanchette et al., JCAP 03, 021 (2023)

- Errors introduced from Maxwellian velocity distribution modeling are much smaller than those from using the underdense empirical density profiles.

Integrated J-factors

Sculptor analogue

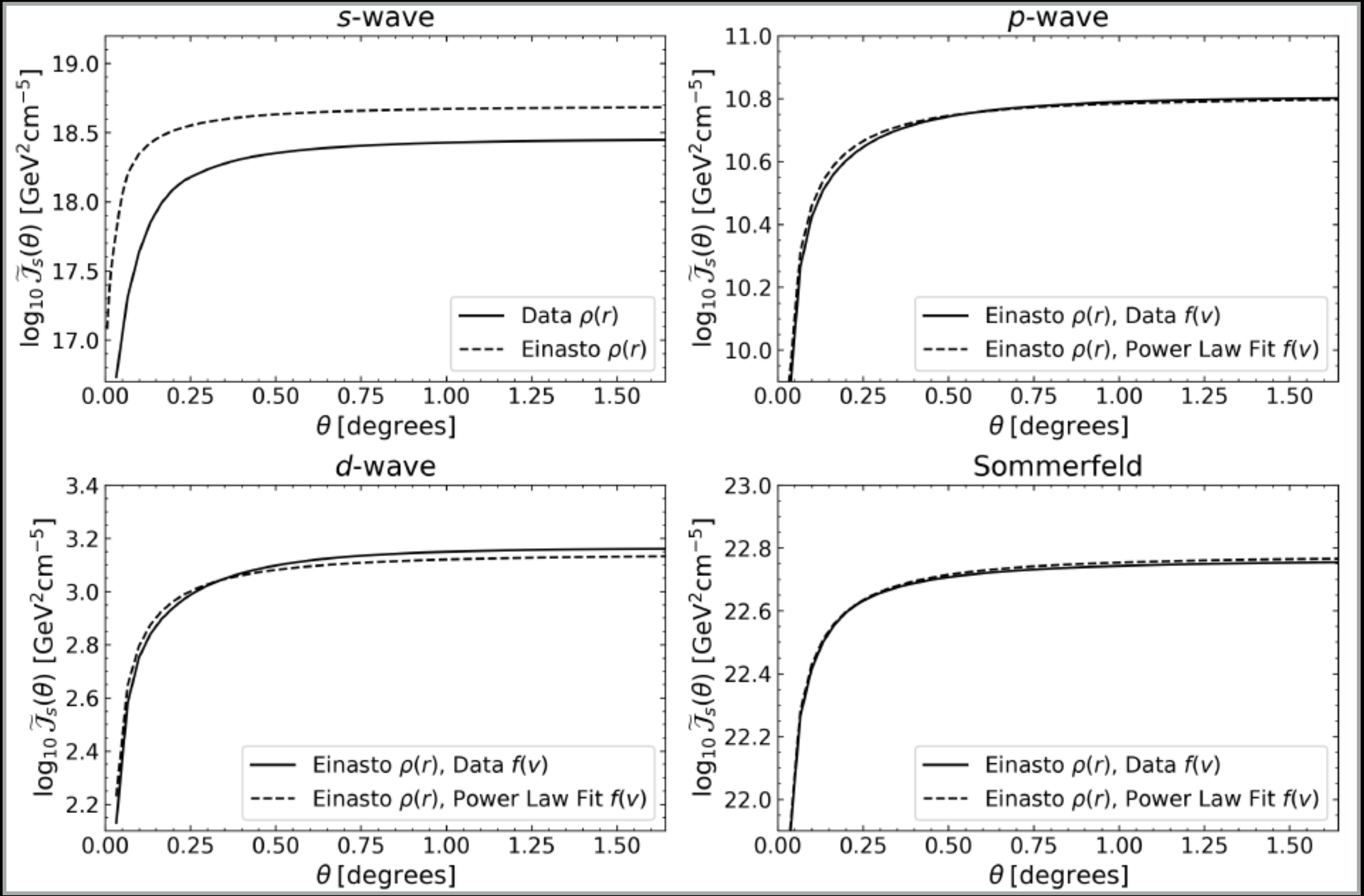

Blanchette et al., JCAP 03, 021 (2023)

- Using the power law to compute the J-factors significantly reduces computation time, and introduces a ~13% error on average for the velocity-dependent models.

Integrated J-factors

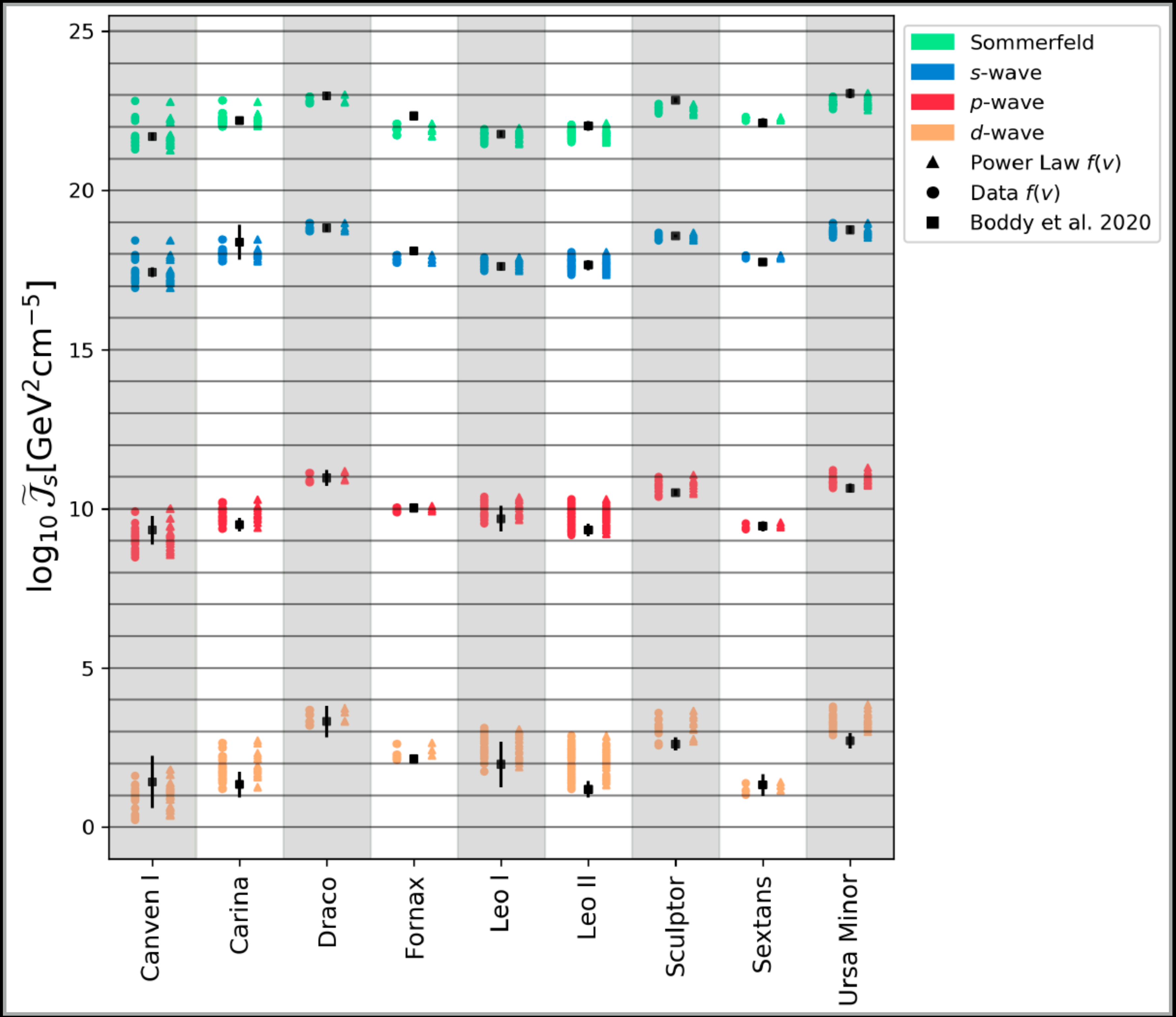

Blanchette et al., JCAP 03, 021 (2023)

Integrated J-factors

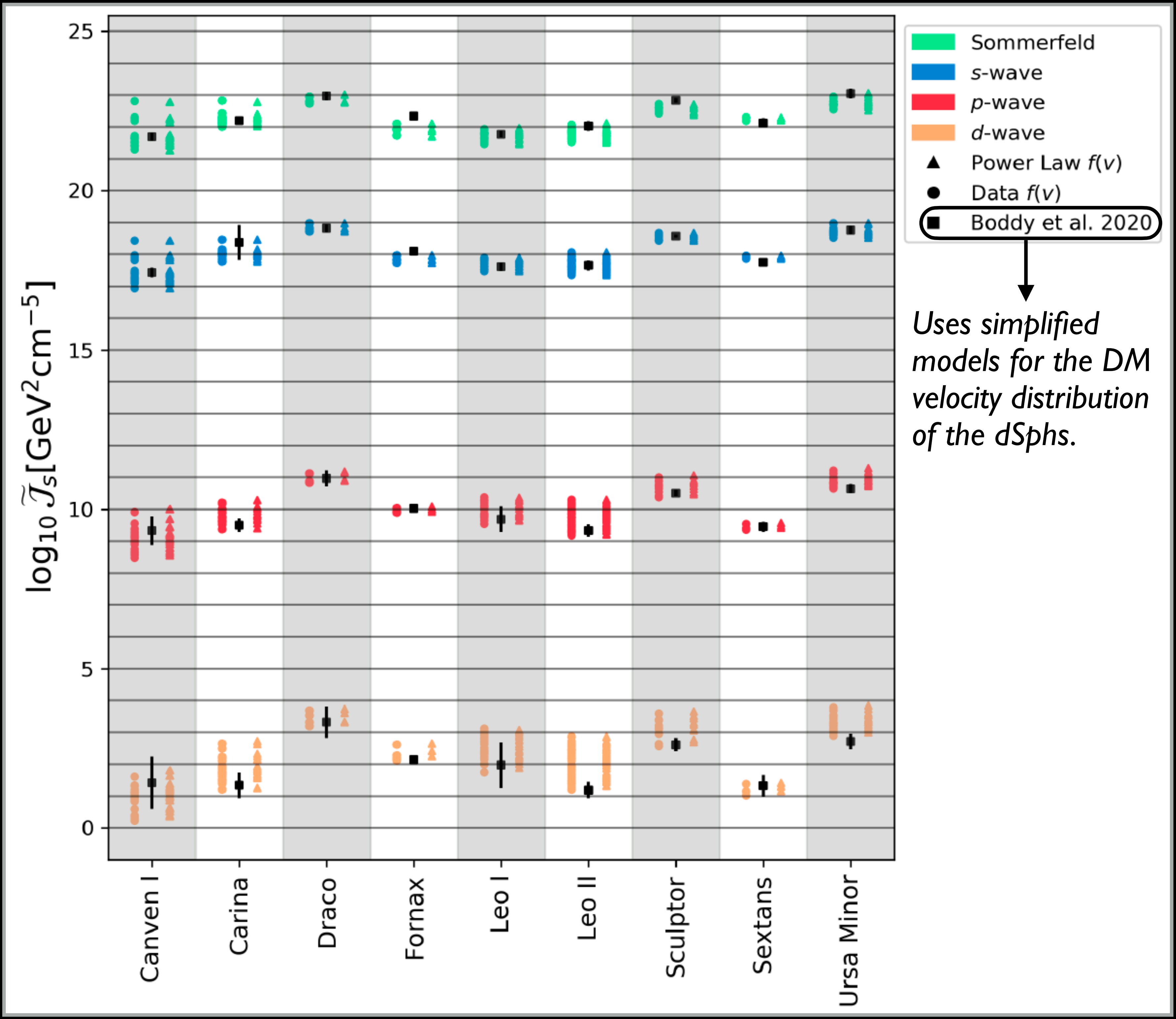

- Our results generally agree with previous work based on simplified models.

Blanchette et al., JCAP 03, 021 (2023)

Integrated J-factors

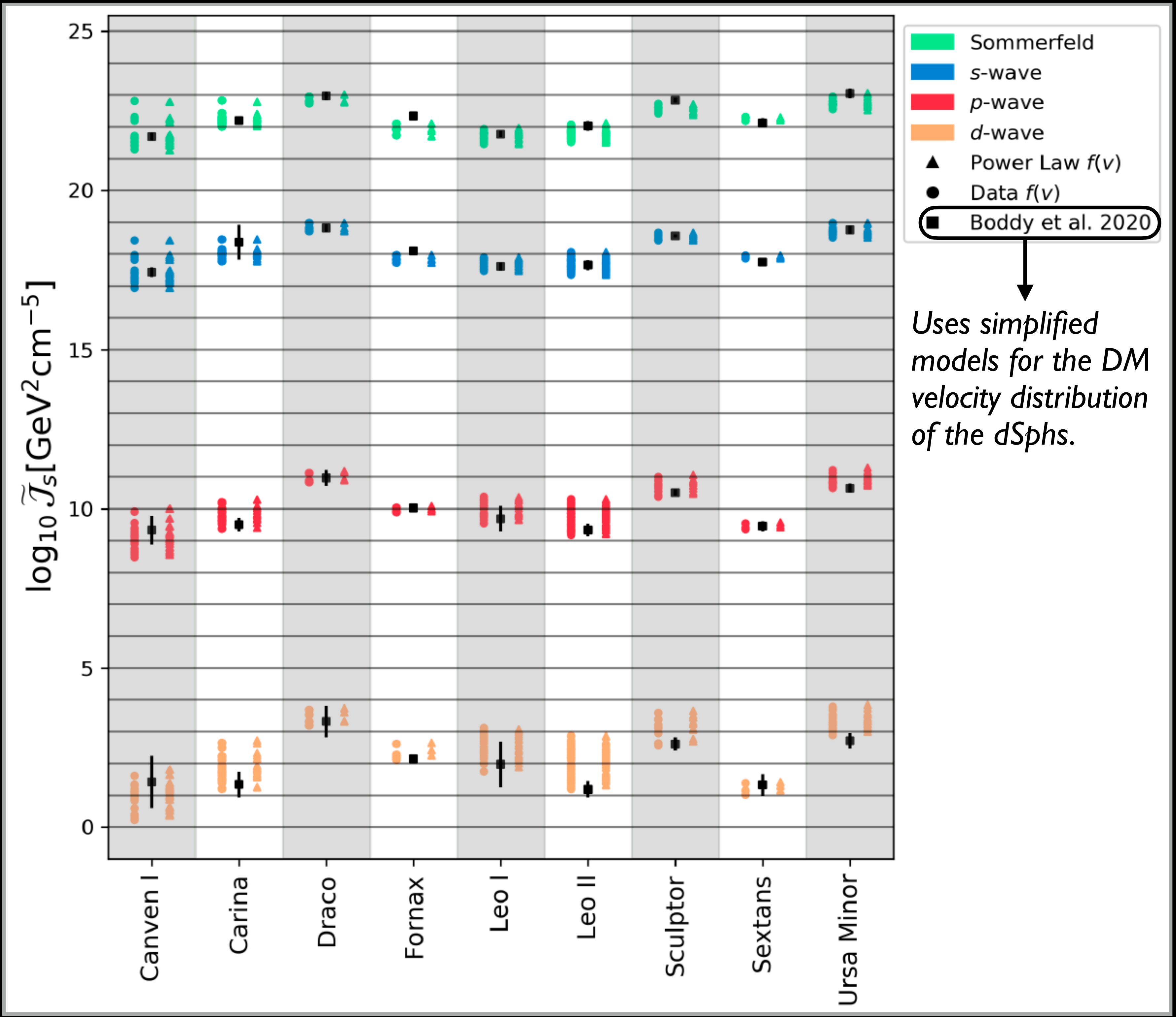

- Our results generally agree with previous work based on simplified models.
- *Halo-to-halo scatter in the J-factors dominate the astrophysical uncertainties.*

Blanchette et al., JCAP 03, 021 (2023)

Dark matter distribution in dSphs

Use **high resolution cosmological simulations** to extract the DM distribution in dSphs.

1. *What is the impact of DM distribution modeling on annihilation signals in Milky Way dSphs?*

Blanchette et al., JCAP 03, 021 (2023)

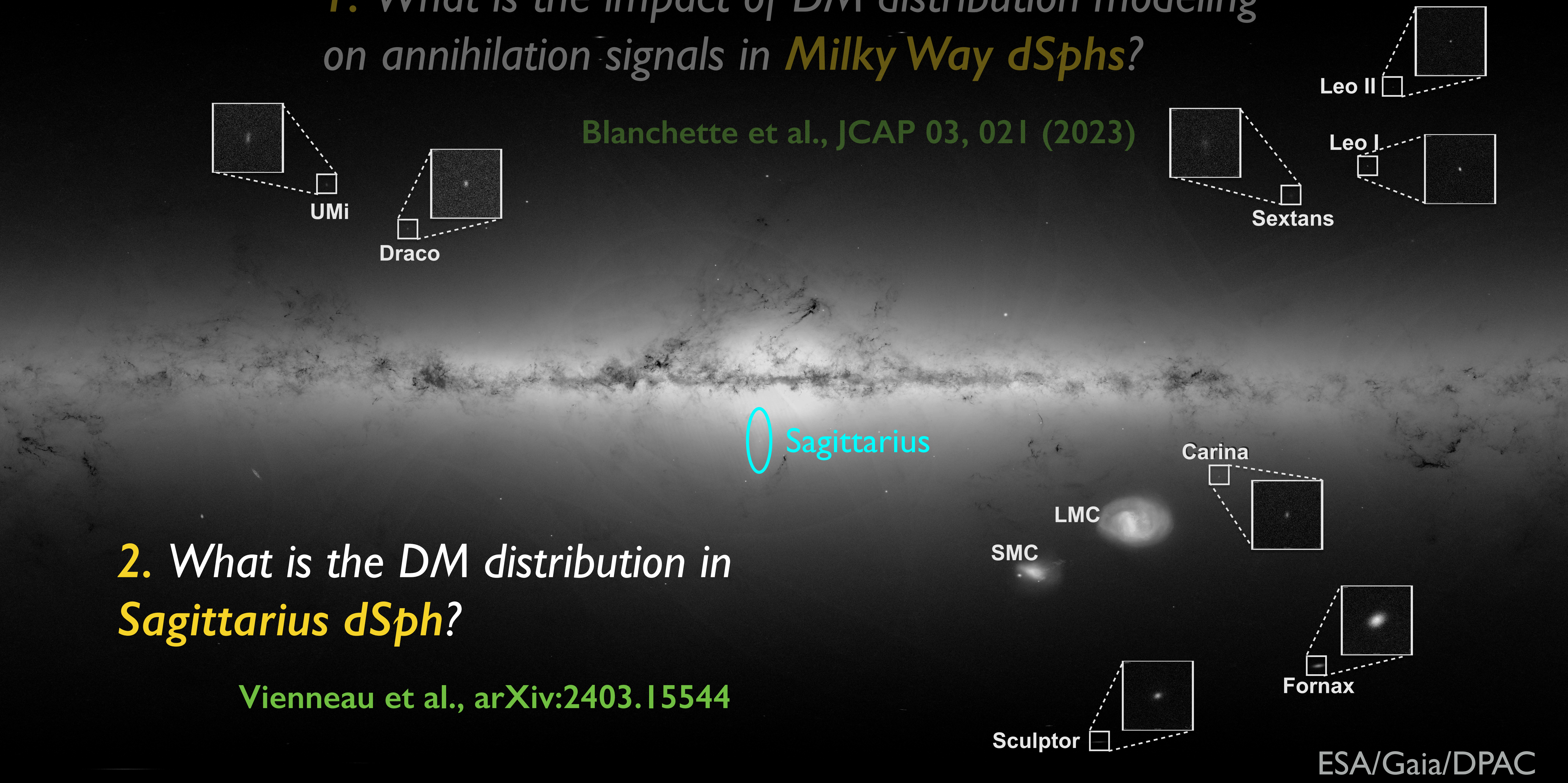

2. *What is the DM distribution in Sagittarius dSph?*

Vienneau et al., arXiv:2403.15544

Sagittarius

- Sagittarius is one of the most unique dSphs of the Milky Way. It is DM dominated, but also has a population of globular clusters.

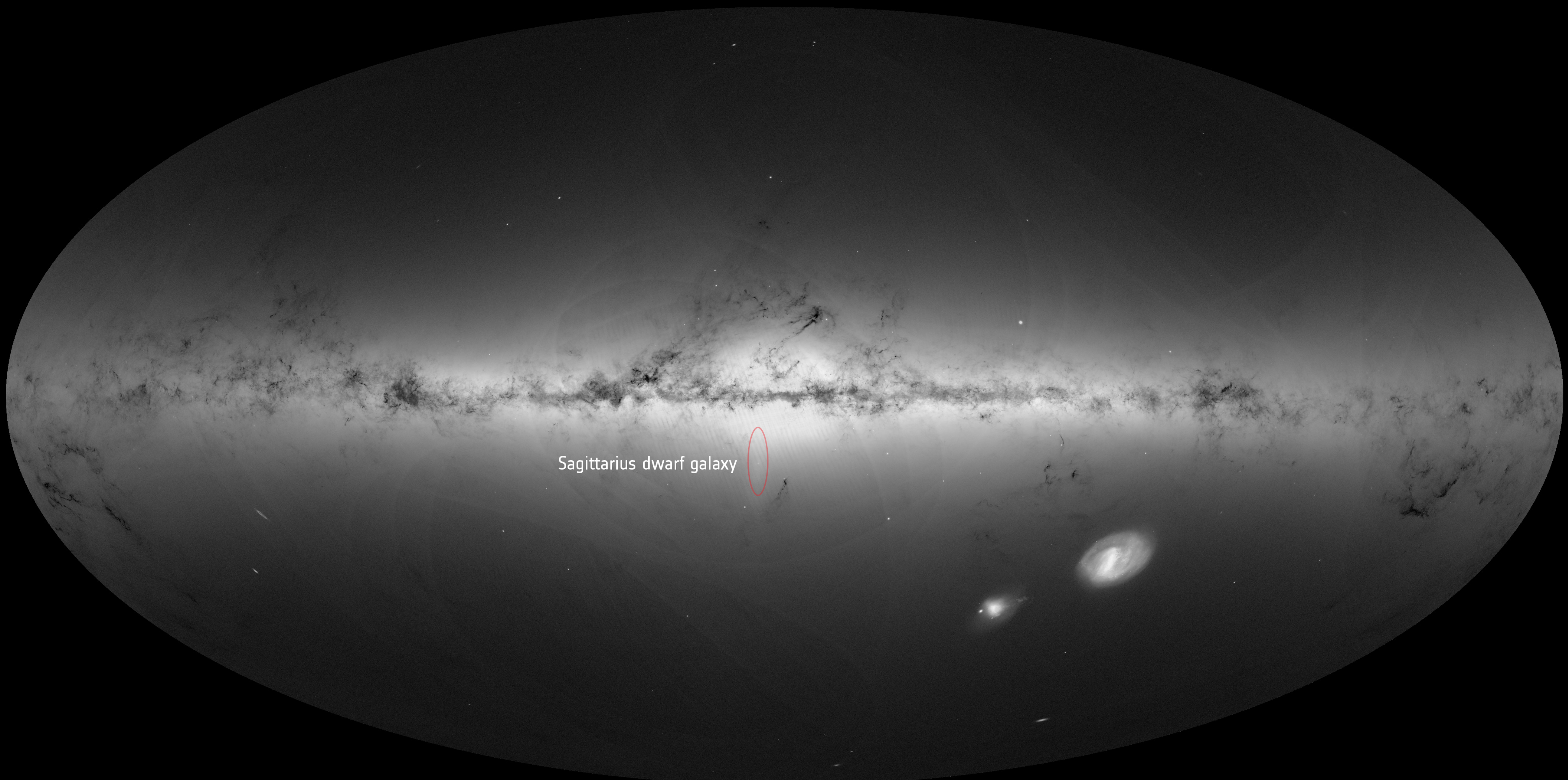

ESA/Gaia/DPAC

Sagittarius

- Sagittarius is one of the most unique dSphs of the Milky Way. It is DM dominated, but also has a population of globular clusters.

- Recently, a gamma-ray source identified in Fermi-LAT data coincident with location of M54, the globular cluster at the center of Sagittarius.

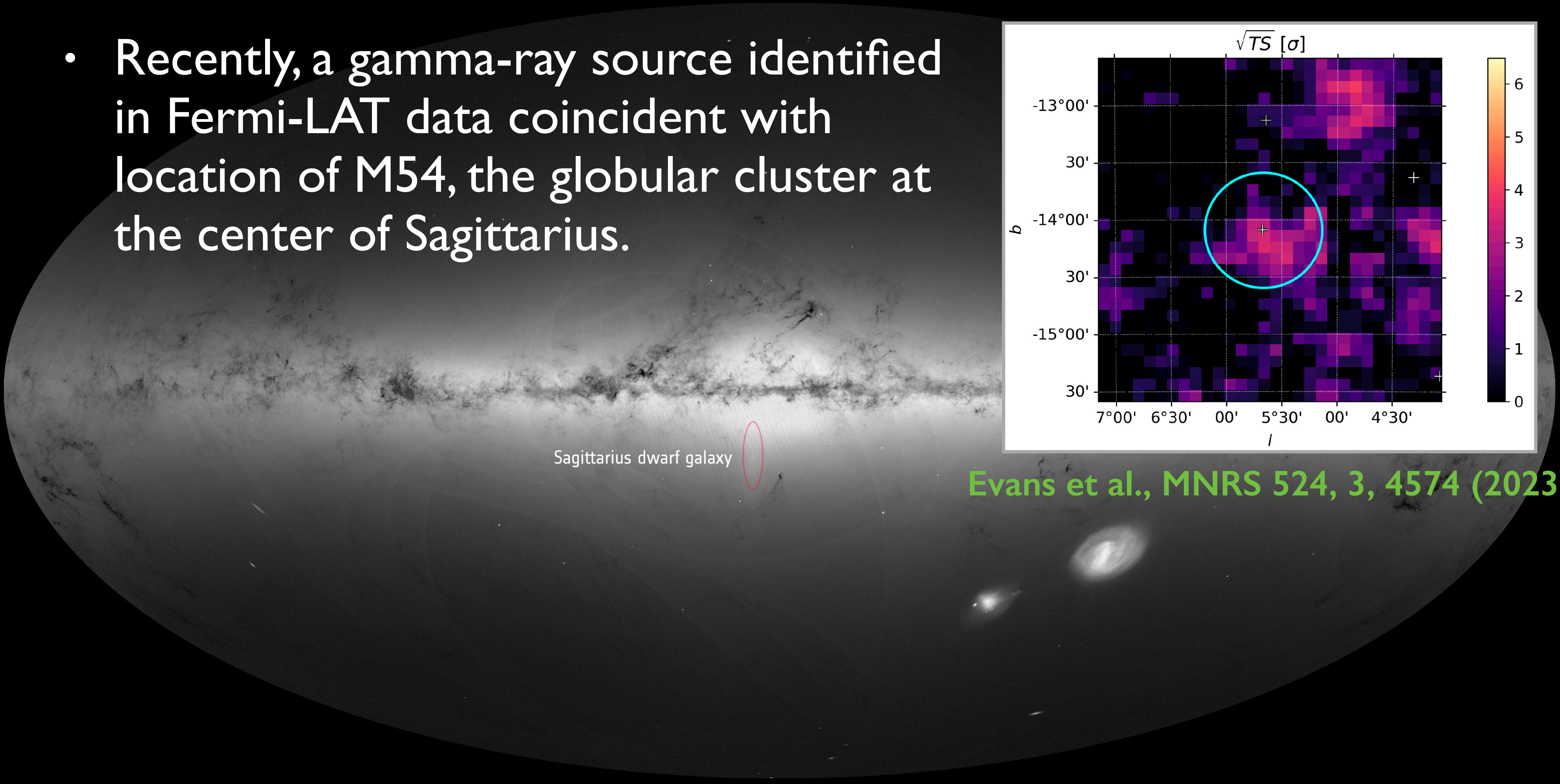

Evans et al., MNRS 524, 3, 4574 (2023)

ESA/Gaia/DPAC

Sagittarius

- Sagittarius is one of the most unique dSphs of the Milky Way. It is DM dominated, but also has a population of globular clusters.

- Recently, a gamma-ray source identified in Fermi-LAT data coincident with location of M54, the globular cluster at the center of Sagittarius. → *Consistent with either a millisecond pulsar or a DM interpretation*

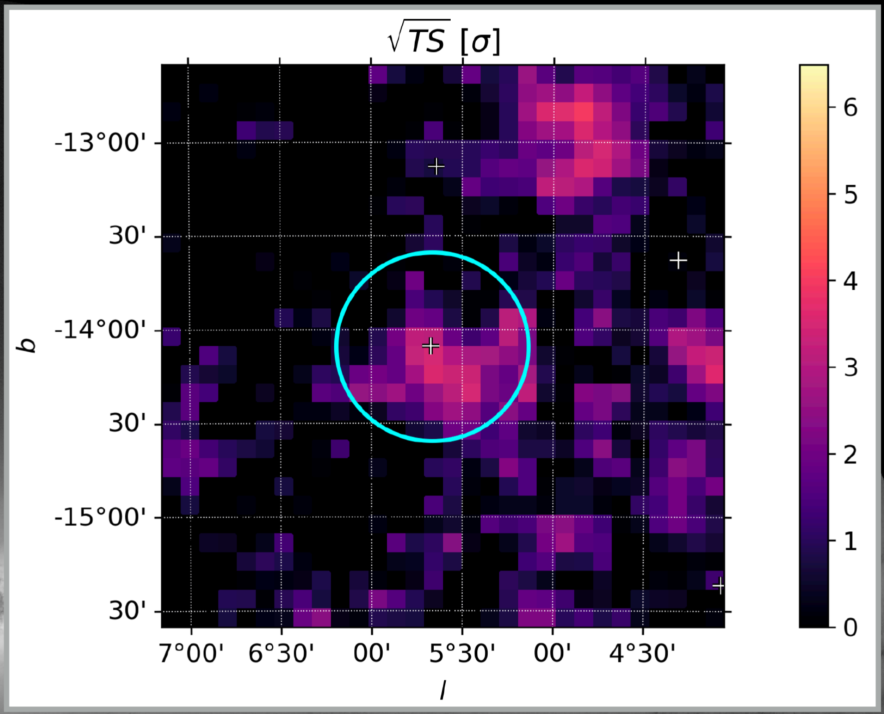

Evans et al., MNRS 524, 3, 4574 (2023)

Sagittarius dwarf galaxy

ESA/Gaia/DPAC

Sagittarius

- Sagittarius is one of the most unique dSphs of the Milky Way. It is DM dominated, but also has a population of globular clusters.

- Recently, a gamma-ray source identified in Fermi-LAT data coincident with location of M54, the globular cluster at the center of Sagittarius. → *Consistent with either a millisecond pulsar or a DM interpretation*

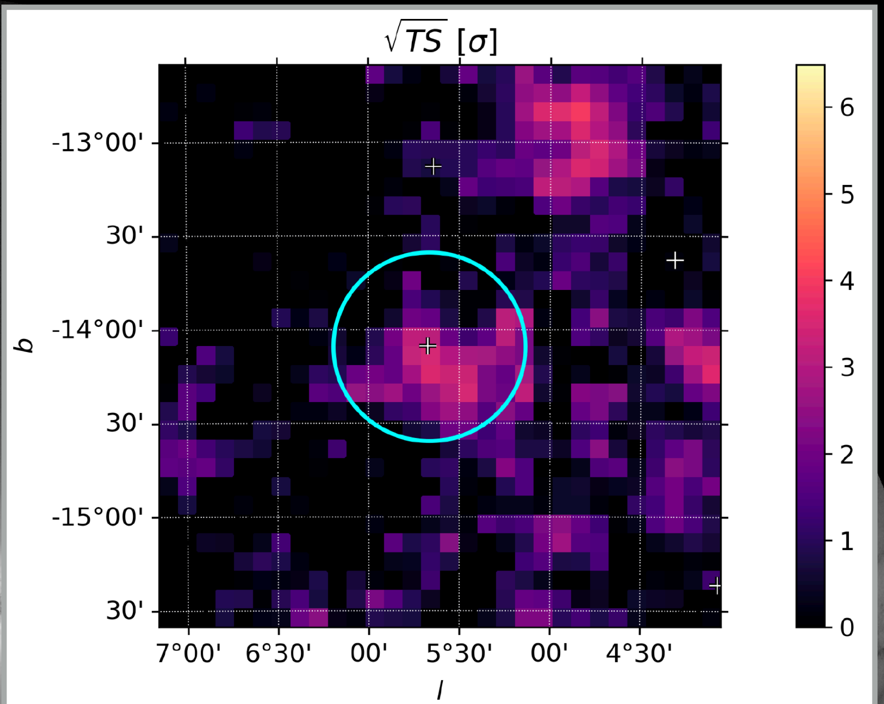

Evans et al., MNRS 524, 3, 4574 (2023)

Crucial to accurately model the DM distribution in Sagittarius.

ESA/Gaia/DPAC

Sagittarius

Important properties of Sagittarius:

- Relatively nearby (~ 26 kpc from Sun) → High gamma-ray flux expected from DM annihilation.

- Just below the Galactic Center → Milky Way DM halo can contribute significantly to the DM annihilation signal.

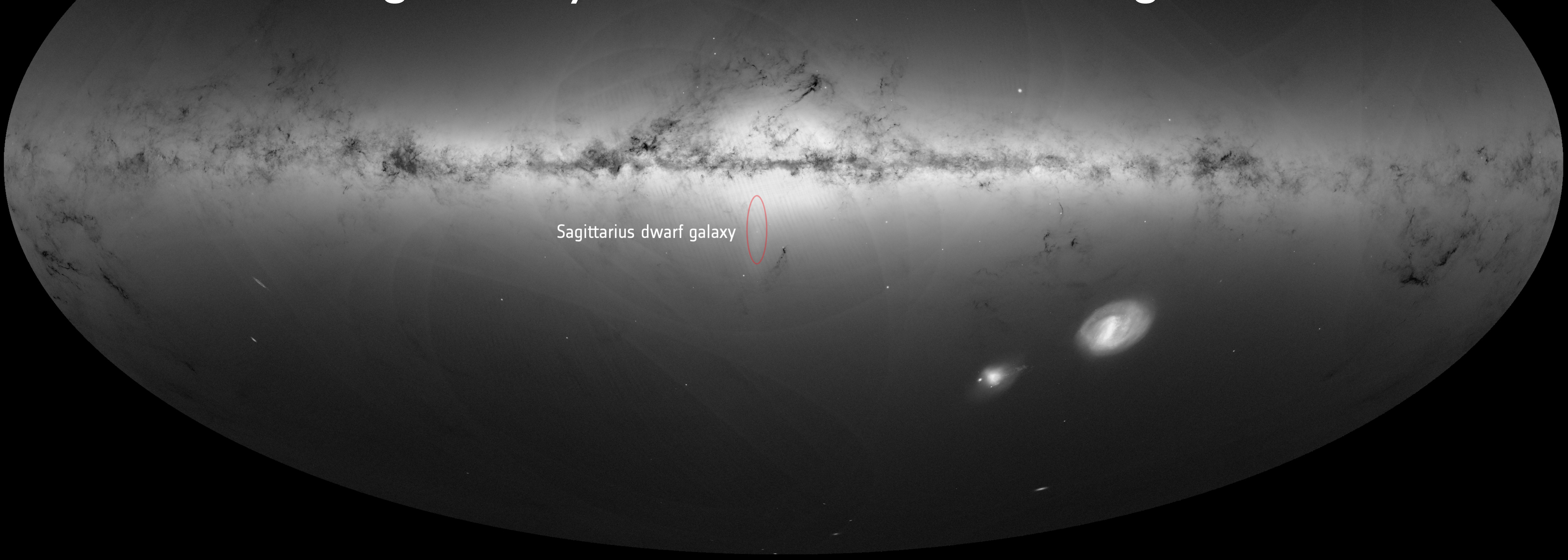

ESA/Gaia/DPAC

Auriga cosmological simulations

- State-of-the-art cosmological magneto-hydrodynamical zoom-in simulations of Milky Way size halos.

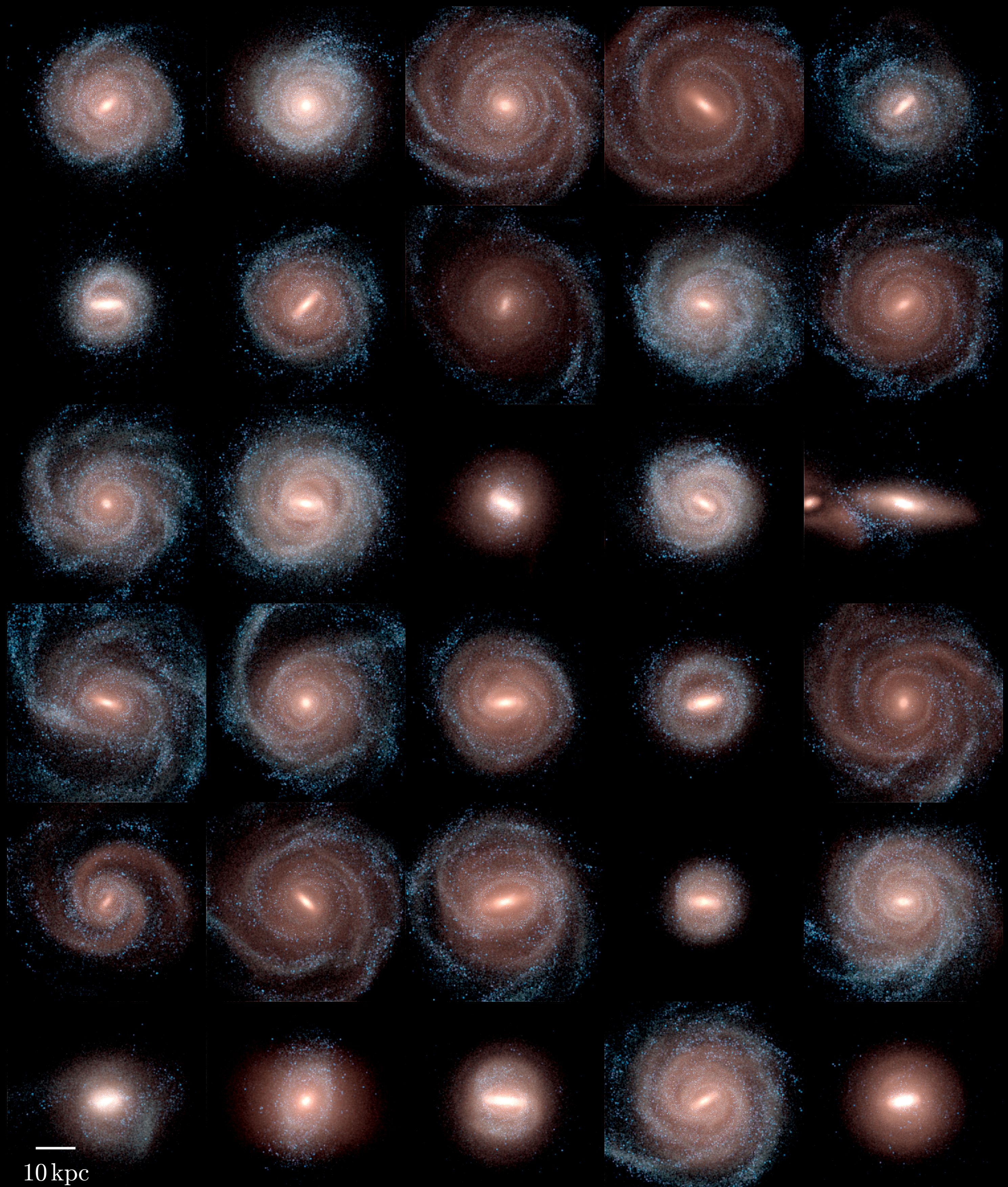

Auriga cosmological simulations

- State-of-the-art cosmological magneto-hydrodynamical zoom-in simulations of Milky Way size halos.

- 6 Milky Way analogues at the high resolution level:

$m_{\rm DM}$ [$M_\odot$]	$m_{\rm b}$ [$M_\odot$]	ϵ [pc]
4×10^4	5×10^3	184

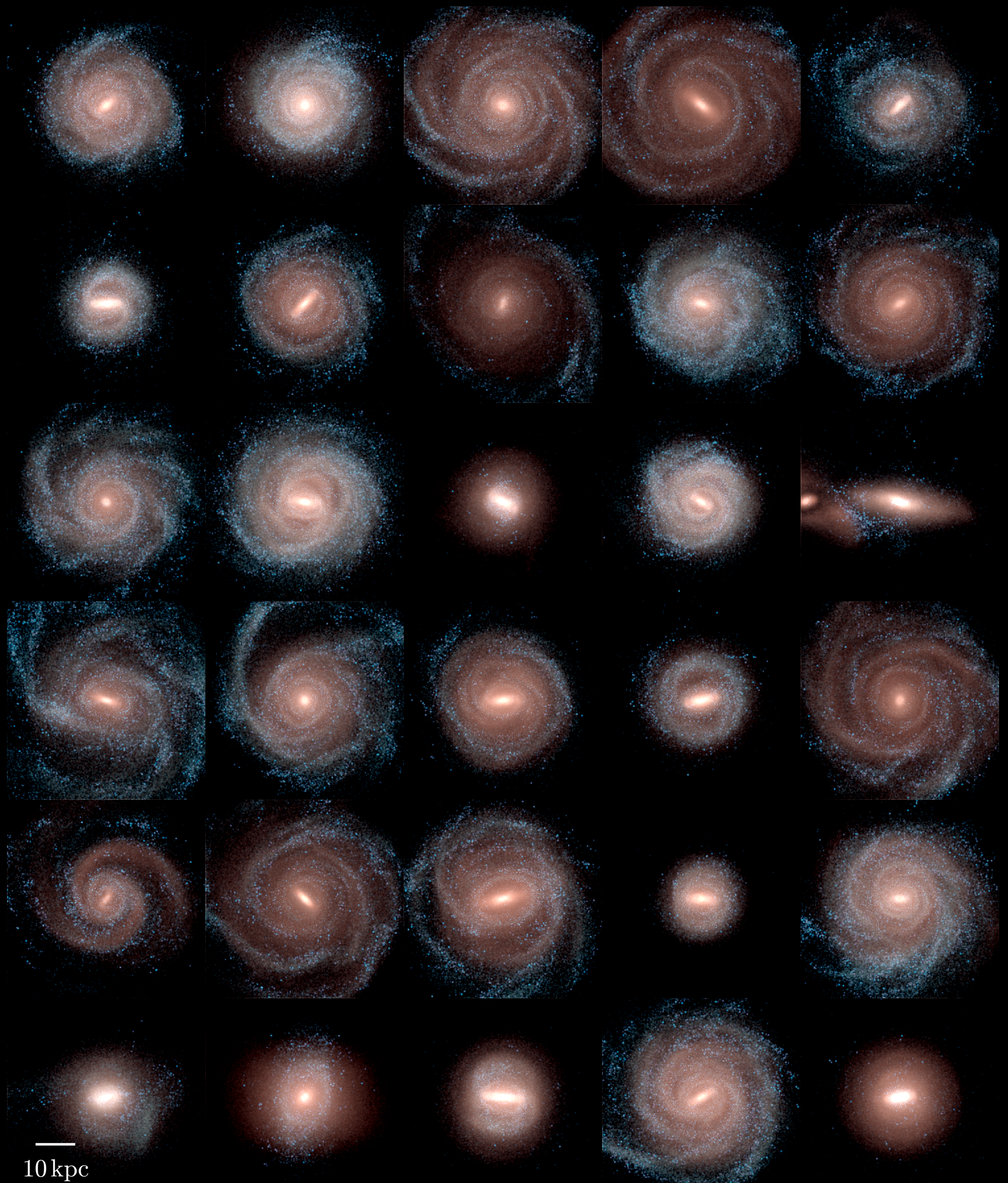

Auriga cosmological simulations

- State-of-the-art cosmological magneto-hydrodynamical zoom-in simulations of Milky Way size halos.

- 6 Milky Way analogues at the high resolution level:

m_{DM} [$M_\odot$]	m_b [$M_\odot$]	ϵ [pc]
4×10^4	5×10^3	184

- Identify **6 Sagittarius analogues** based on their stellar mass and distance from host galaxy.

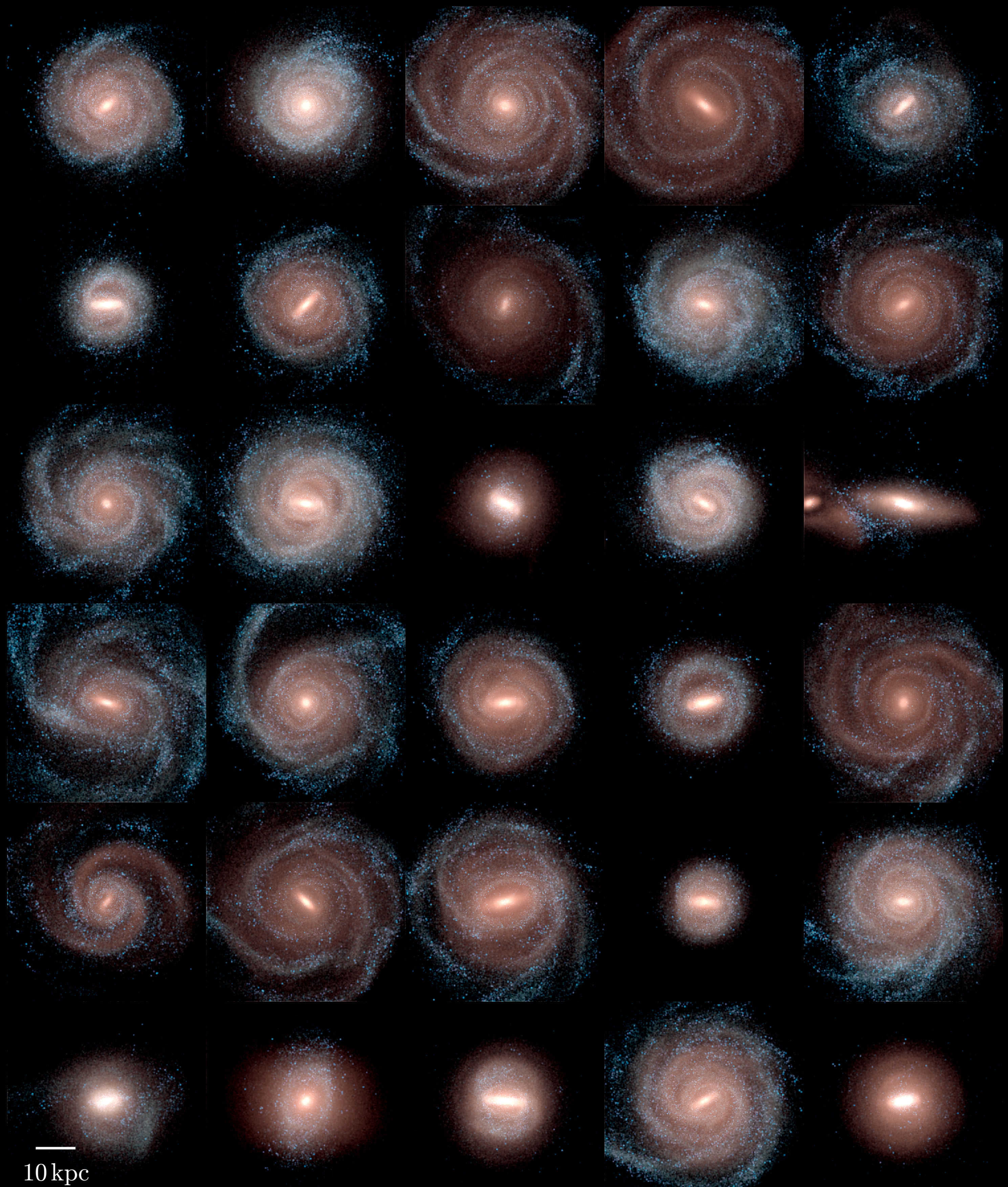

Dark matter distribution

- Consider for the first time the contribution of Milky Way DM particles that spatially overlap with Sagittarius, but are not bound to it → *Unbound particles*

Dark matter distribution

- Consider for the first time the contribution of Milky Way DM particles that spatially overlap with Sagittarius, but are not bound to it ➡ ***Unbound particles***

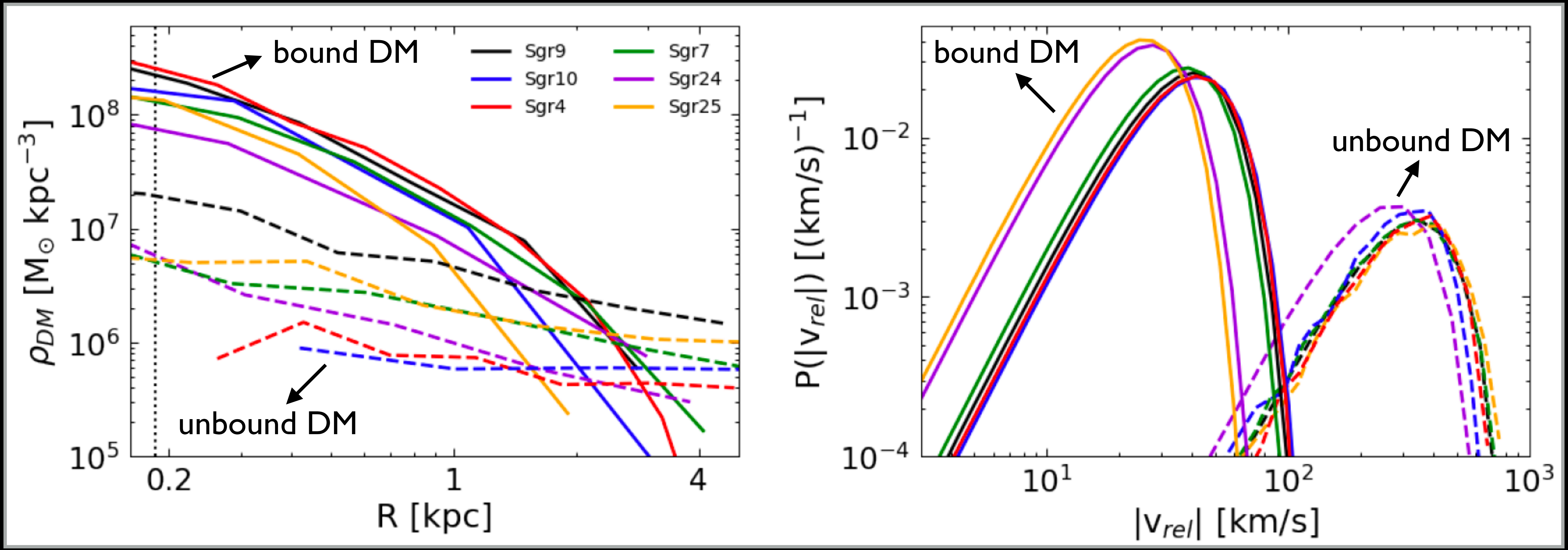

Vienneau et al., arXiv:2403.15544

Dark matter distribution

- Consider for the first time the contribution of Milky Way DM particles that spatially overlap with Sagittarius, but are not bound to it → *Unbound particles*

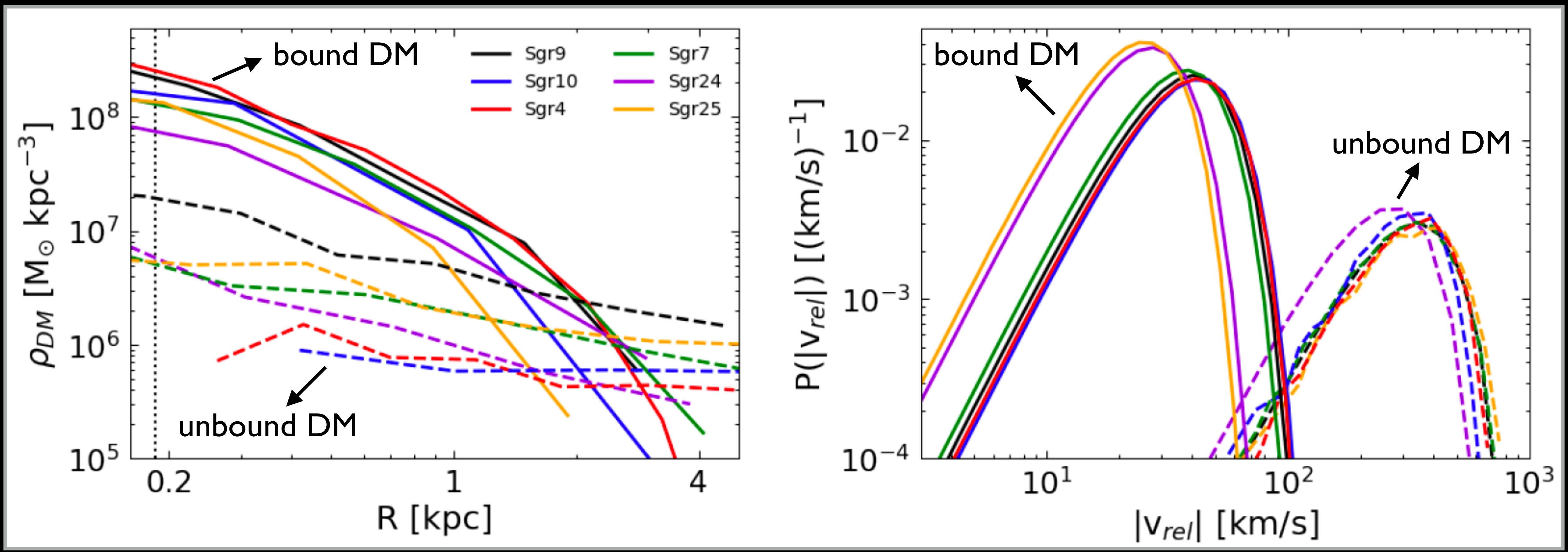

Vienneau et al., arXiv:2403.15544

- *Higher peak speeds for unbound DM particles compared to bound DM.*

Dark matter distribution

- Consider for the first time the contribution of Milky Way DM particles that spatially overlap with Sagittarius, but are not bound to it → *Unbound particles*

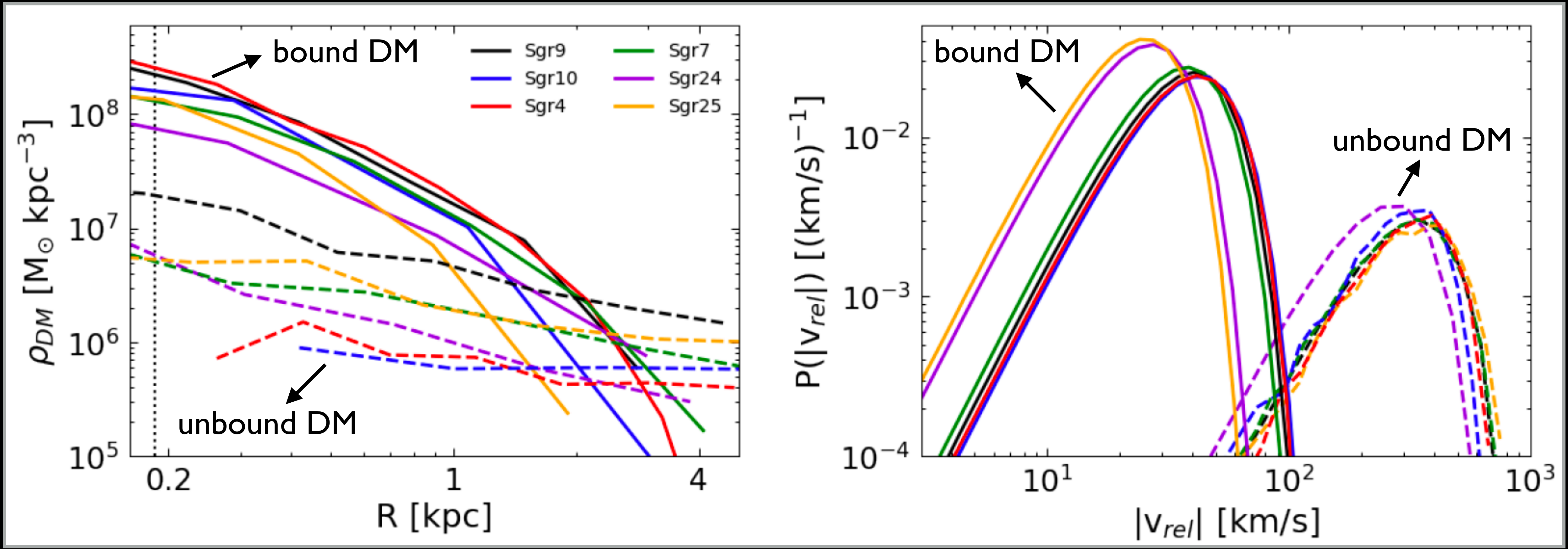

Vienneau et al., arXiv:2403.15544

- *Higher peak speeds for unbound DM particles compared to bound DM.* → Expected since speed of Milky Way DM at the position of Sagittarius is larger than speed of DM bound to Sagittarius.

J-factors

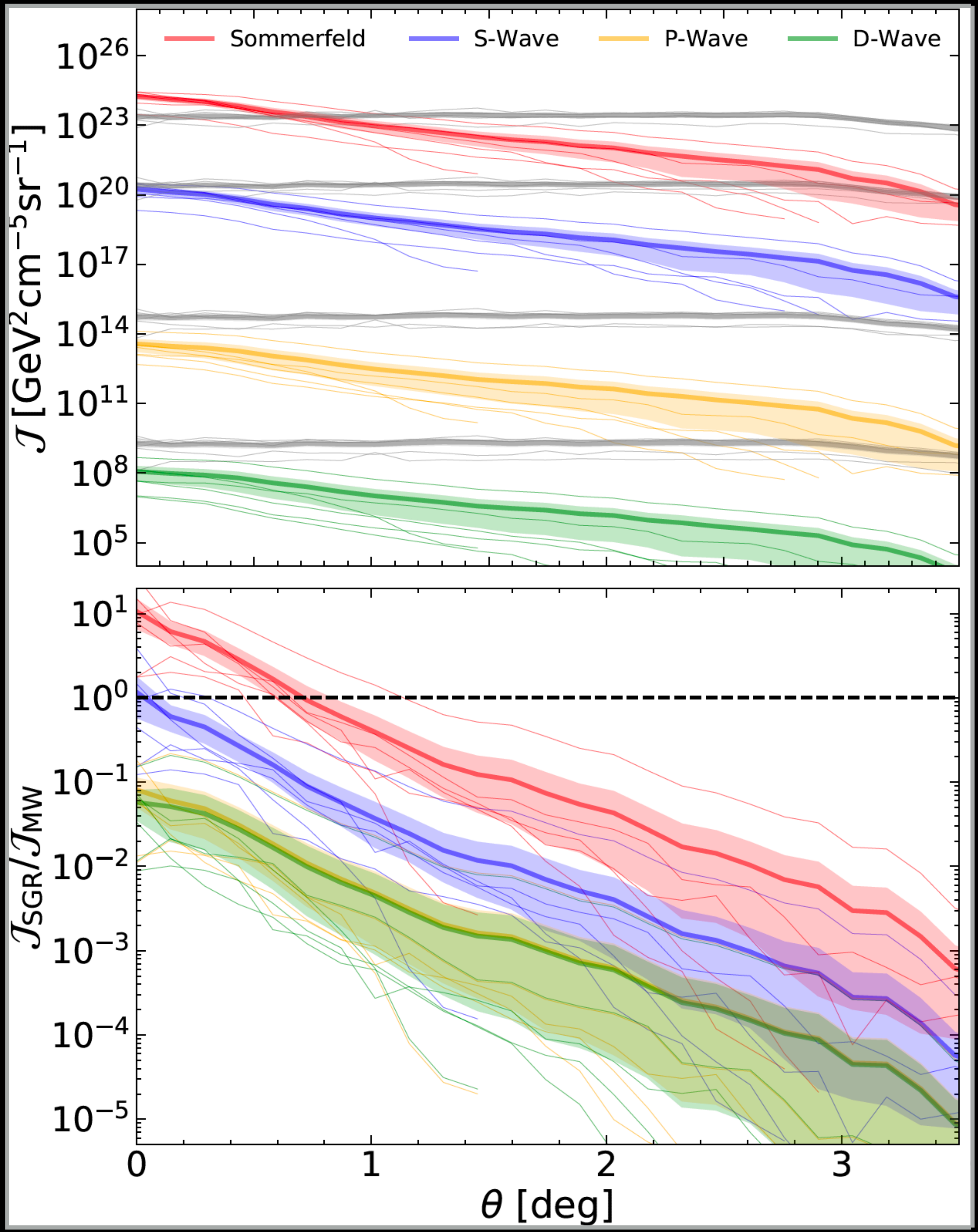

Vienneau et al., arXiv:2403.15544

J-factors

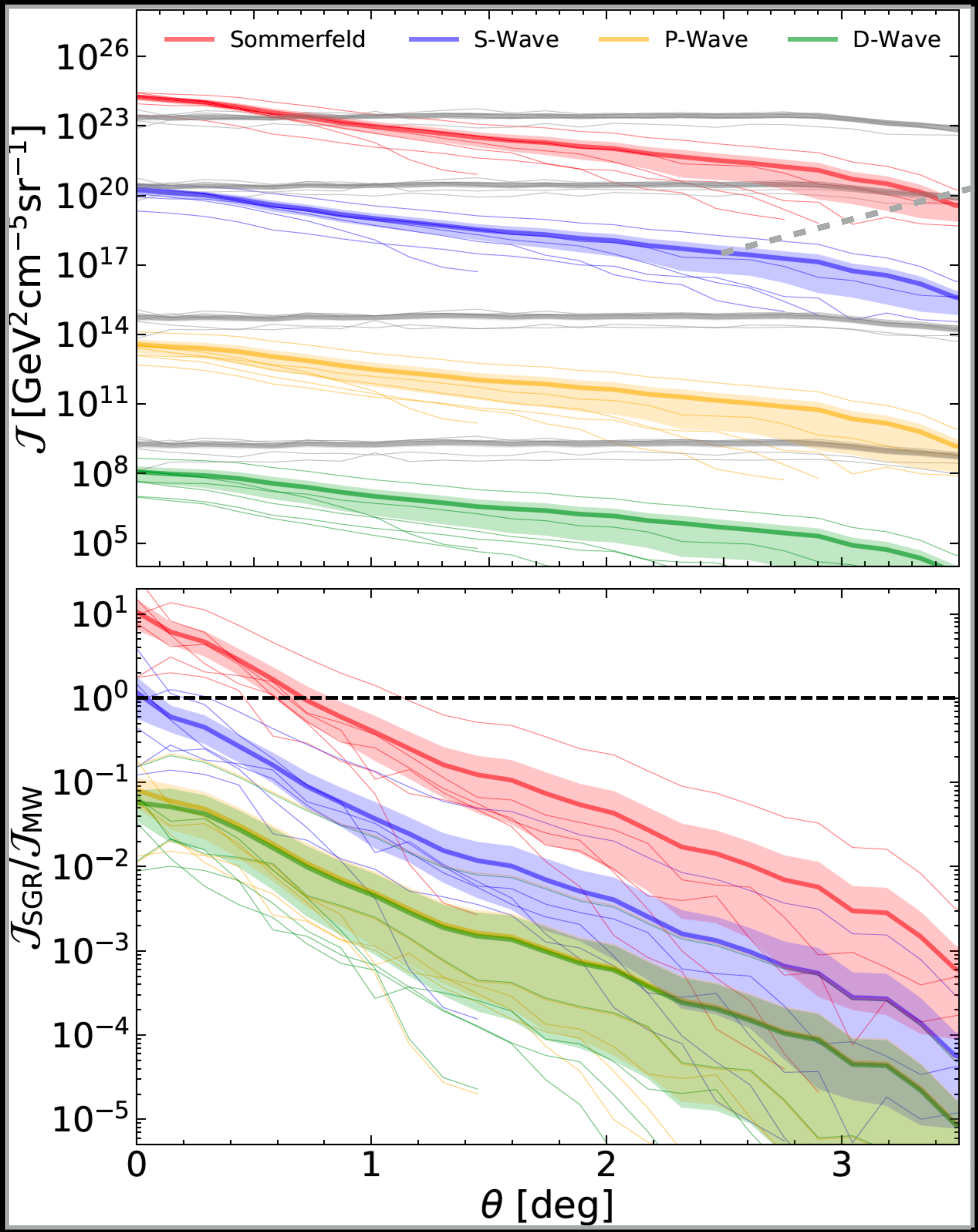

Colored: J-factors of the Sagittarius analogue (bound + unbound)

Vienneau et al., arXiv:2403.15544

J-factors

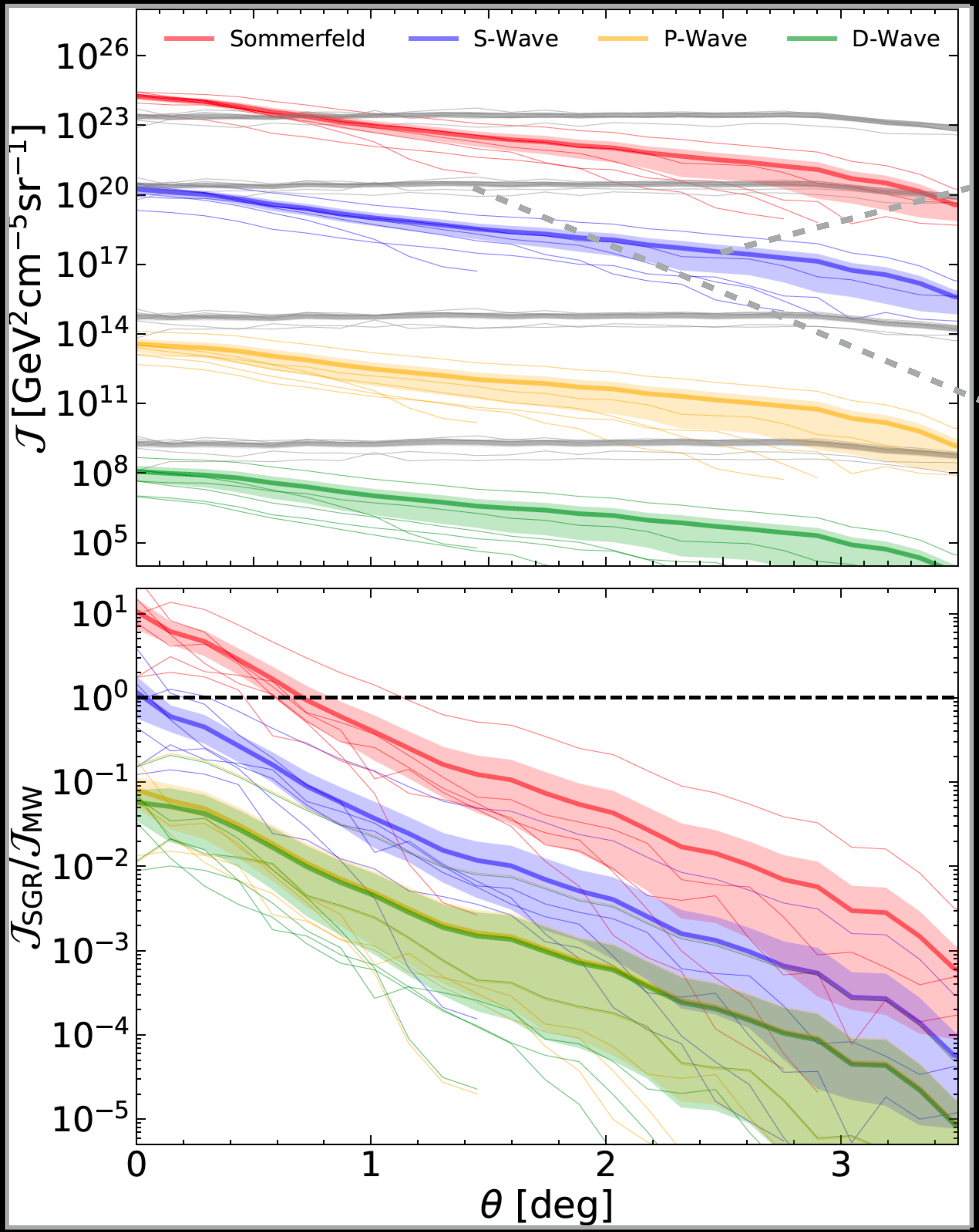

Colored: J-factors of the Sagittarius analogue (bound + unbound)

Grey: J-factors of the host Milky Way halo along the line-of-sight to the Sagittarius analogue

Vienneau et al., arXiv:2403.15544

J-factors

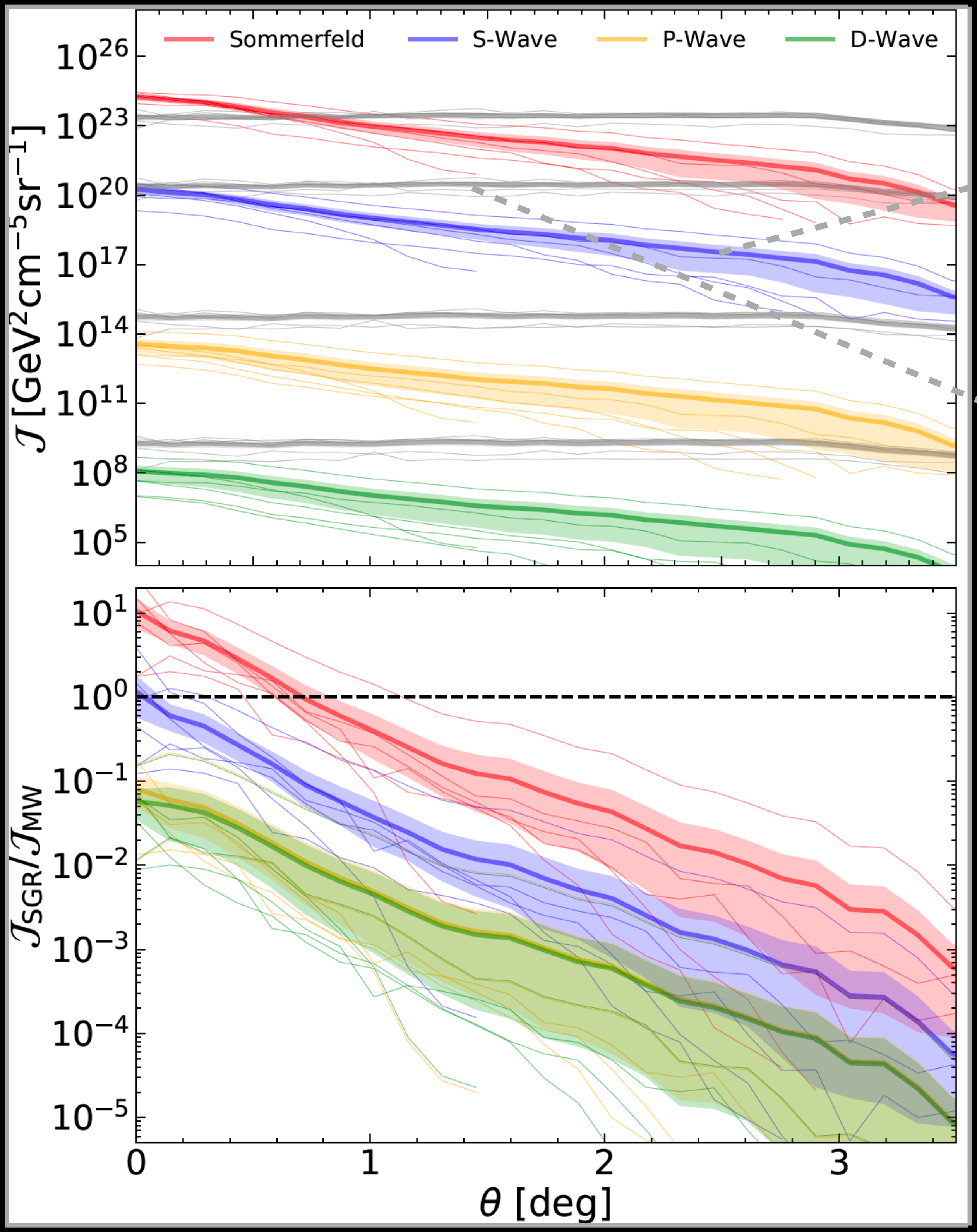

Vienneau et al., arXiv:2403.15544

Colored: J-factors of the Sagittarius analogue (bound + unbound)

Grey: J-factors of the host Milky Way halo along the line-of-sight to the Sagittarius analogue

- The Milky Way diffuse signal dominates the Sagittarius signal in all cases, except for the Sommerfeld case.

J-factor maps

Top panels: Sagittarius analogue (bound + unbound)

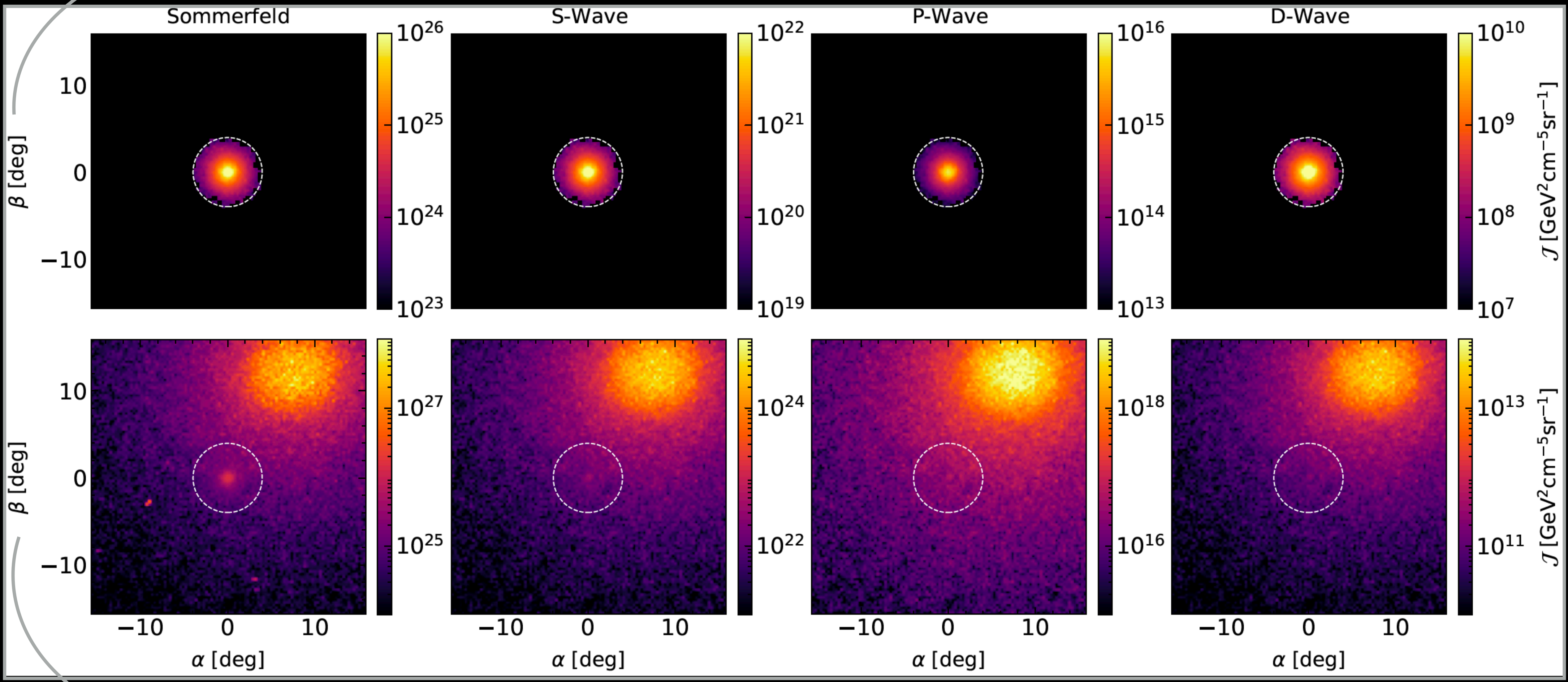

Bottom panels: Entire region (Sagittarius + Milky Way)

J-factor maps

Top panels: Sagittarius analogue (bound + unbound)

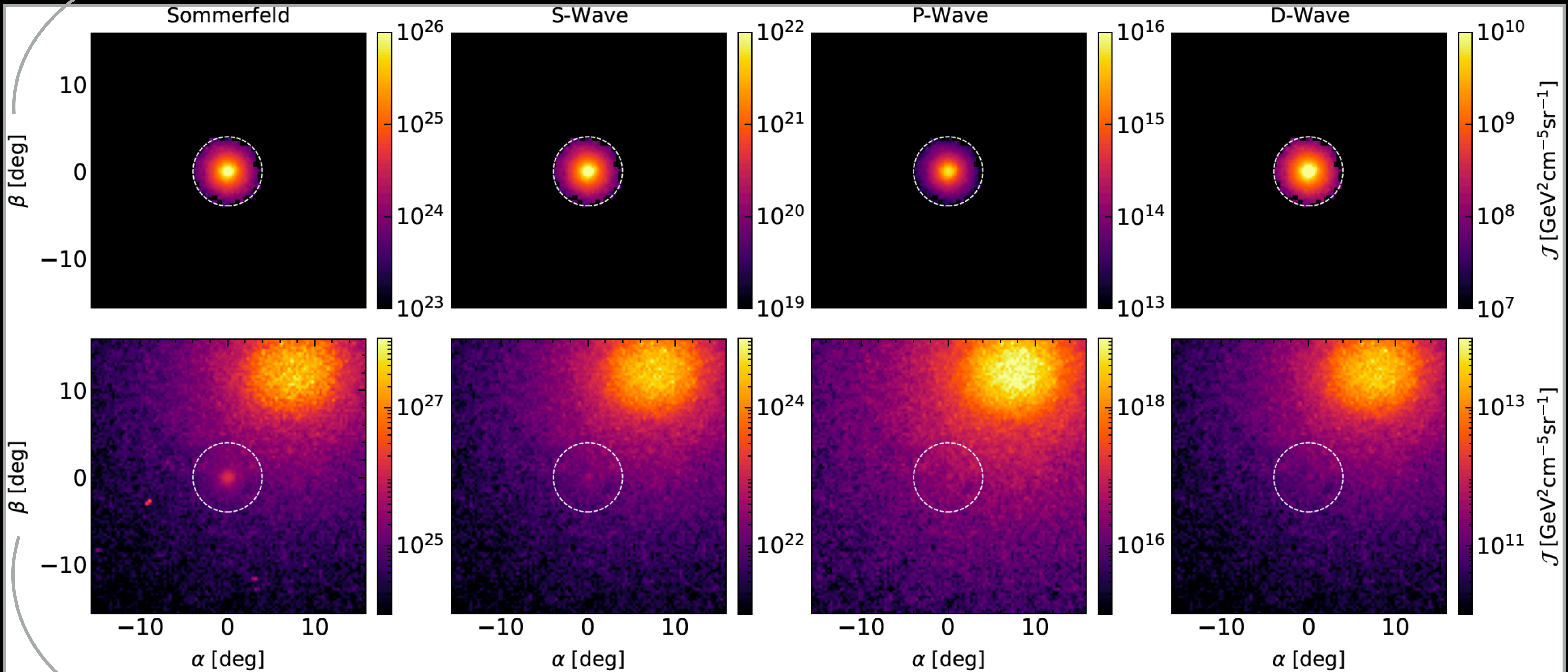

Bottom panels: Entire region (Sagittarius + Milky Way)

- Only in the **Sommerfeld** case, the Sagittarius source is clearly visible above the diffuse Milky Way emission.

Impact of unbound particles

- The **unbound DM** particles that reside in the spatial region of specific dSphs are generally not included in the analysis of DM annihilation signals. → *They become important for velocity-dependent annihilation.*

Impact of unbound particles

- The **unbound DM** particles that reside in the spatial region of specific dSphs are generally not included in the analysis of DM annihilation signals. → *They become important for velocity-dependent annihilation.*

- Compare the **true J-factors computed from bound+unbound DM particles** in the Sagittarius analogues to the unphysical case of emission from **only DM particles bound to Sagittarius.**

Impact of unbound particles

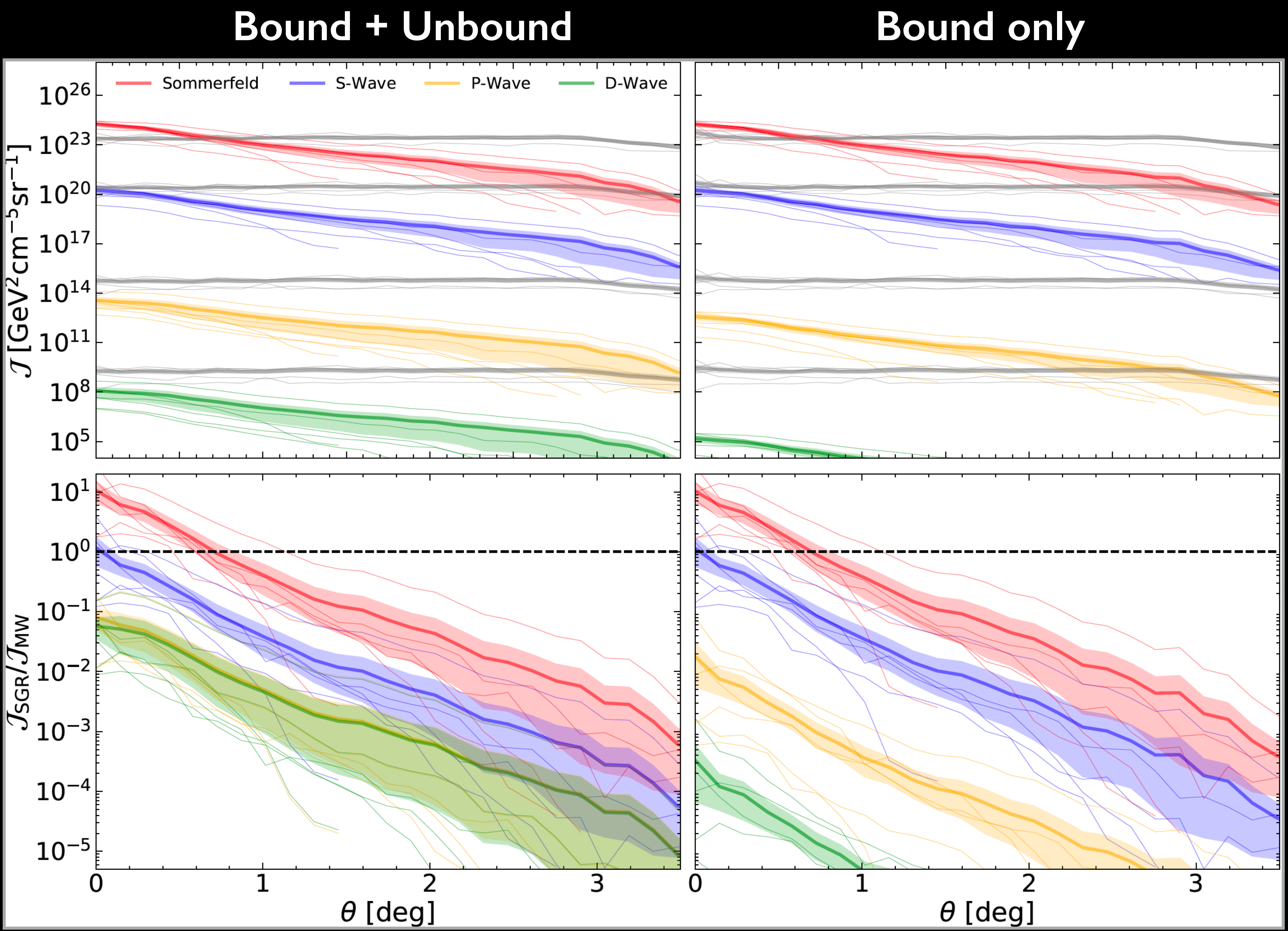

Vienneau et al., arXiv:2403.15544

Impact of unbound particles

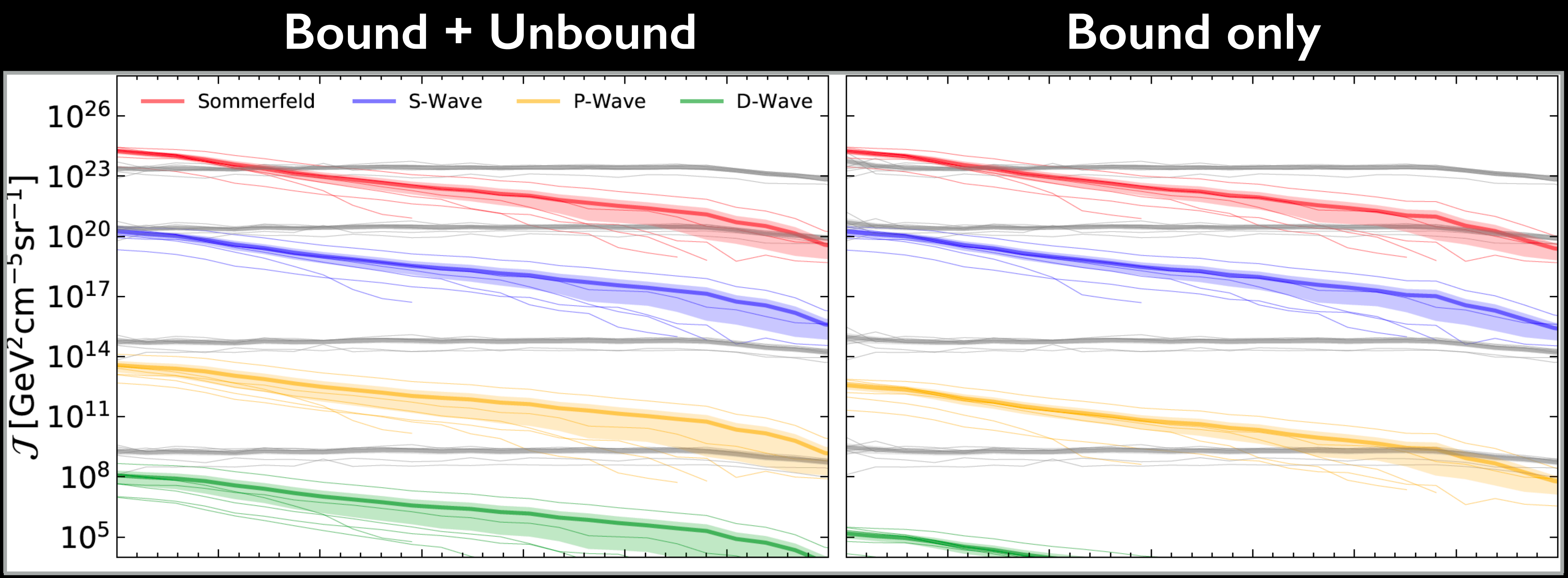

- The unbound DM particles modify the Sagittarius J-factors:
  - **p-wave:** *increase by up to a factor 40*
  - **d-wave:** *increase by up to 4 orders of magnitude*
  - **Sommerfeld:** *minimal change*
  - **s-wave:** *minimal change*

Impact of unbound particles

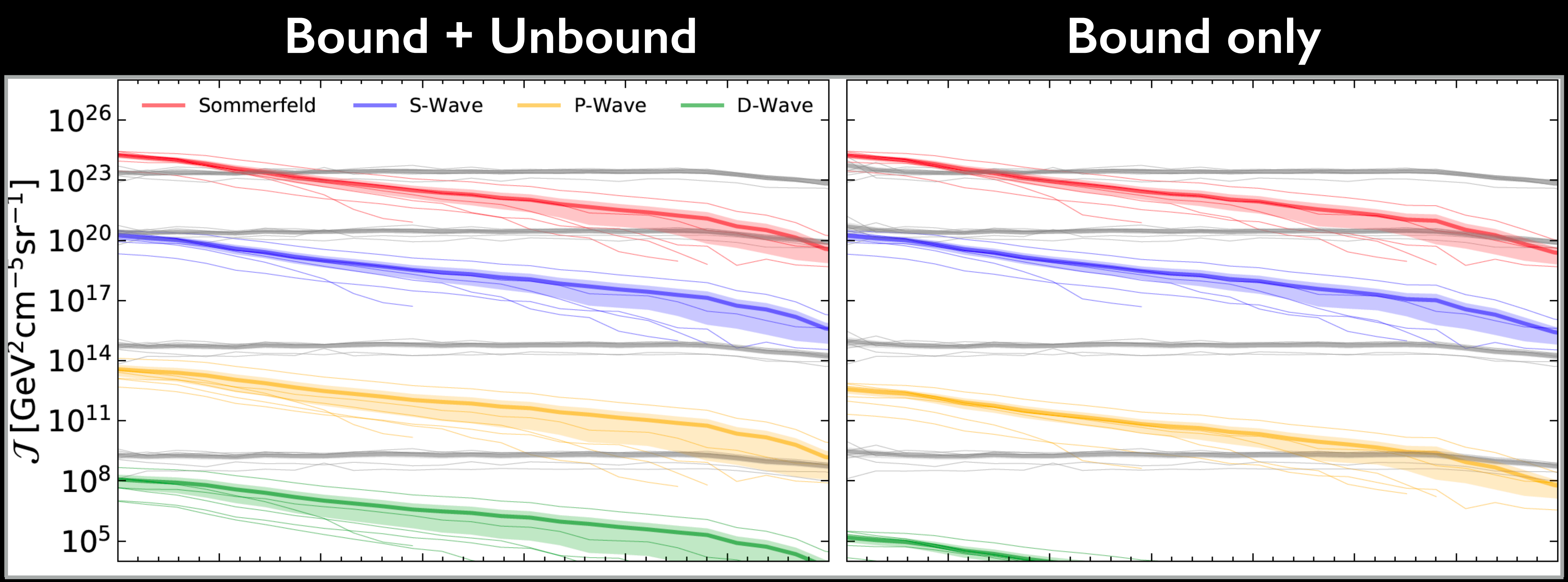

- The unbound DM particles modify the Sagittarius J-factors:
  - **p-wave:** *increase by up to a factor 40*
  - **d-wave:** *increase by up to 4 orders of magnitude*
  - **Sommerfeld:** *minimal change*
  - **s-wave:** *minimal change*
- *Modifications due to annihilation of the unbound DM particles with themselves and with the bound DM particles in Sagittarius.*

Summary

Cosmological simulations can be used to accurately model the DM distribution in dSphs. → *Accurate predictions for indirect DM searches*

Summary

Cosmological simulations can be used to accurately model the DM distribution in dSphs. → *Accurate predictions for indirect DM searches*

General results for dSphs:

- DM relative velocity distributions consistent with Maxwellian at all radii.

Summary

Cosmological simulations can be used to accurately model the DM distribution in dSphs. → *Accurate predictions for indirect DM searches*

General results for dSphs:

- DM relative velocity distributions consistent with Maxwellian at all radii.
- A simple **power-law** relation between the dSph's *maximum circular velocity* and the *Maxwellian peak speed* can be used to accurately model the DM velocity distribution.

Summary

Cosmological simulations can be used to accurately model the DM distribution in dSphs. → *Accurate predictions for indirect DM searches*

General results for dSphs:

- DM relative velocity distributions consistent with Maxwellian at all radii.
- A simple **power-law** relation between the dSph's *maximum circular velocity* and the *Maxwellian peak speed* can be used to accurately model the DM velocity distribution.

Sagittarius dSph:

- Milky Way DM particles at the position of Sagittarius can *significantly modify* the annihilation signal for p-wave and d-wave models.

Summary

Cosmological simulations can be used to accurately model the DM distribution in dSphs. → *Accurate predictions for indirect DM searches*

General results for dSphs:

- DM relative velocity distributions consistent with Maxwellian at all radii.
- A simple **power-law** relation between the dSph's *maximum circular velocity* and the *Maxwellian peak speed* can be used to accurately model the DM velocity distribution.

Sagittarius dSph:

- Milky Way DM particles at the position of Sagittarius can *significantly modify* the annihilation signal for p-wave and d-wave models.
- *Such modification should exist for all subhalos in close proximity to the Galactic Center.*

Backup Slides

Indirect detection constraints

- Strongest bounds from dwarf galaxies observed by Fermi-LAT for $m_\chi \sim 10 - 1000$ GeV, and from H.E.S.S. and HAWC for $m_\chi \gtrsim 1$ TeV. → They assume **s-wave**.

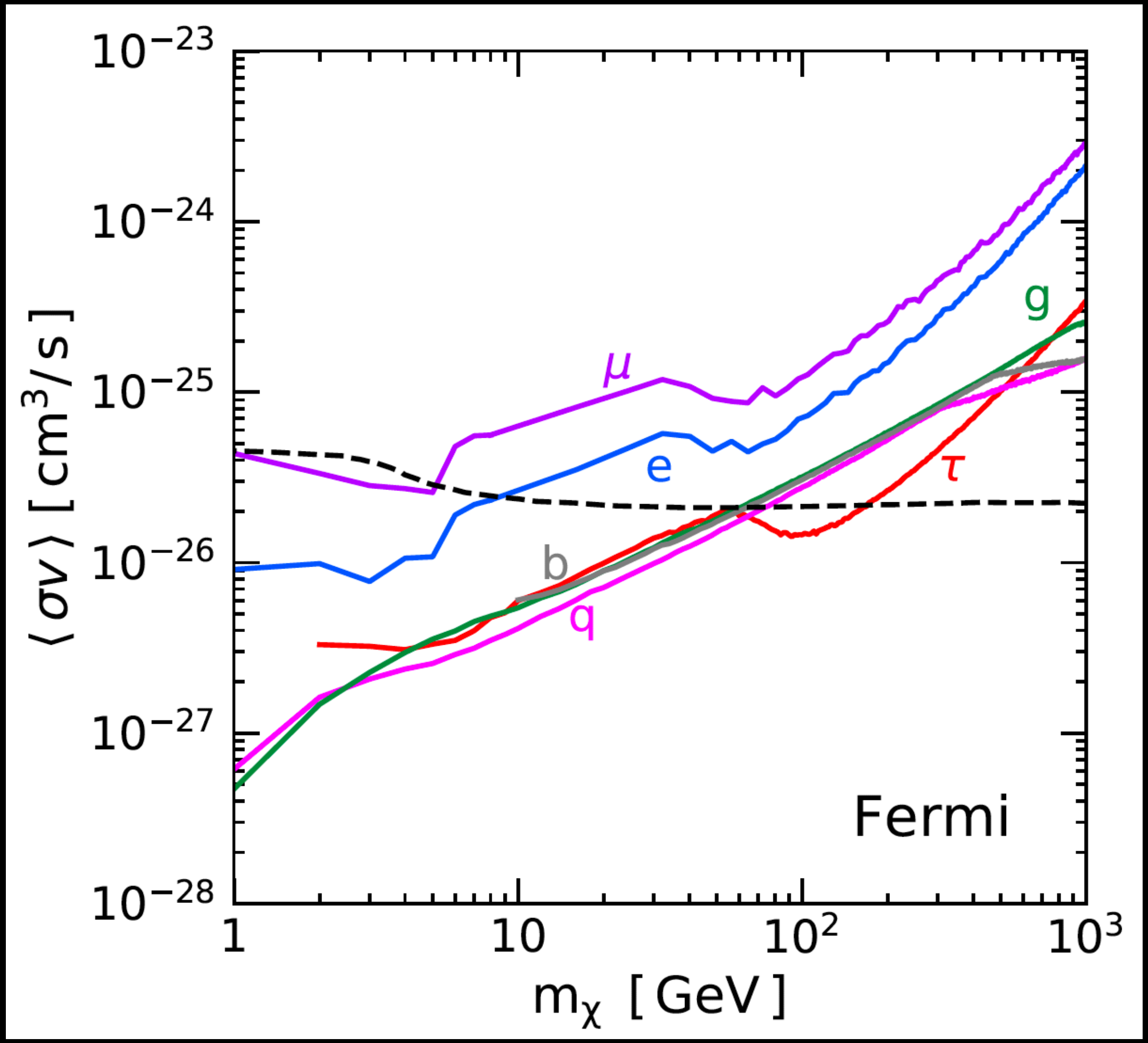

Leane, 2006.00513

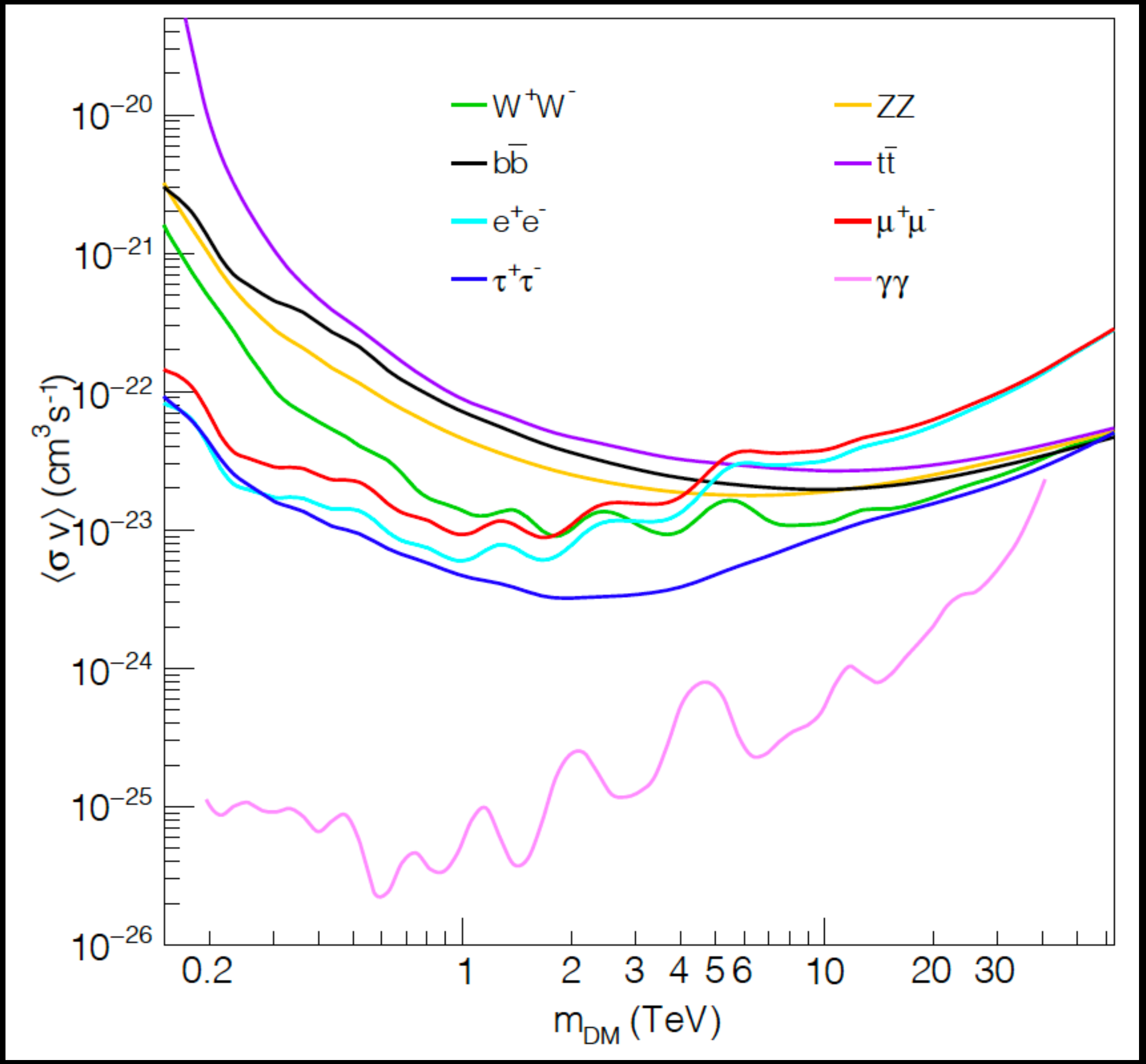

H.E.S.S., 2008.00688

Quantifying modeling errors

- Fitting a Maxwellian in each shell minimizes the errors.

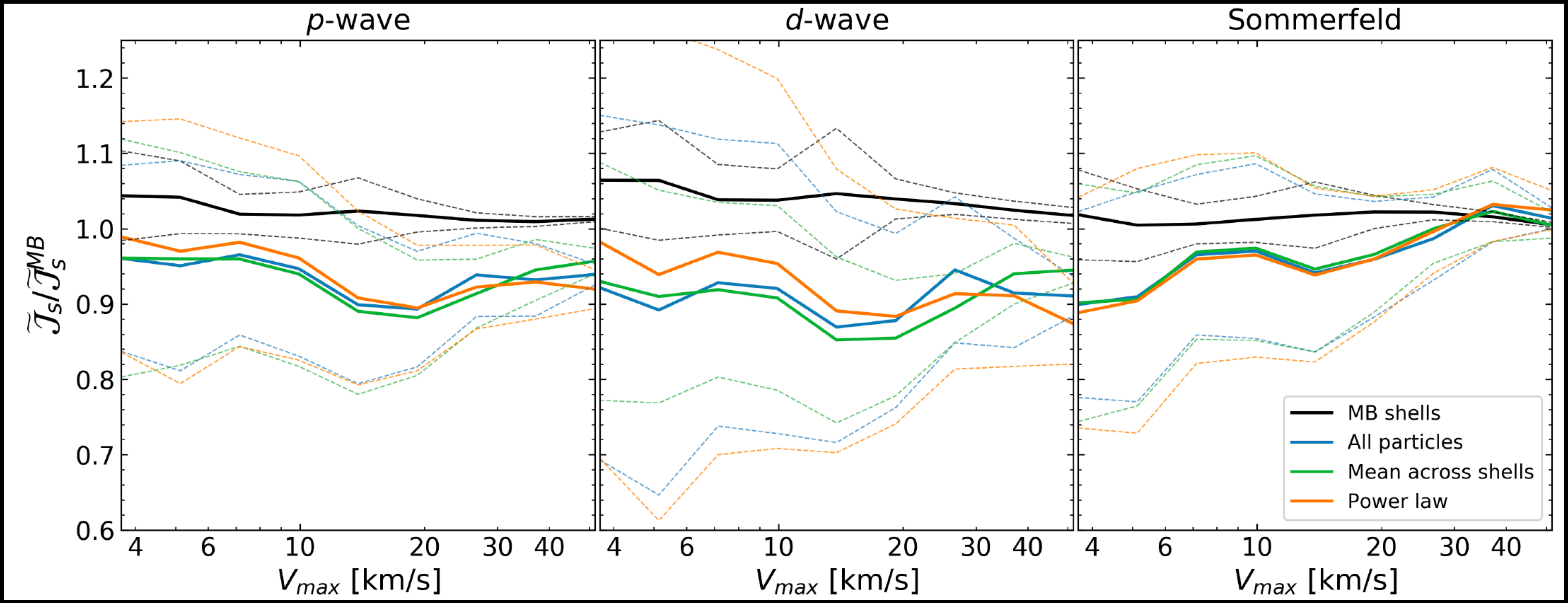

	MB Shells	All particles	Mean across shells	Power law
p-wave	[4.14, 1.25]	[11.24, 6.50]	[12.16, 4.54]	[13.25, 8.82]
d-wave	[5.99, 1.70]	[24.04, 9.92]	[25.30, 5.91]	[26.38, 14.86]
Sommerfeld	[2.00, 1.06]	[12.90, 2.17]	[13.90, 2.45]	[14.43, 2.93]

Blanchette et al., JCAP 03, 021 (2023)

Identifying Sagittarius analogues

- Criteria for identifying Sagittarius analogues: stellar mass in the range of $10^{7.4}\mathrm{M}_\odot < M_* < 10^{8.5}\mathrm{M}_\odot$, and galactocentric distance ≤ 60 kpc. → **6 Sagittarius analogues**

Host name	Dwarf	D [kpc]	$\log_{10}(M_*/\mathrm{M}_\odot)$	$\log_{10}(M_{\mathrm{tot}}/\mathrm{M}_\odot)$	R_{max} [kpc]	Angular size [deg]
Au16	9	28.08	7.933	8.810	1.957	3.945
Au21	10	44.70	8.446	8.780	1.078	1.395
Au23	4	49.01	8.297	8.851	1.583	1.884
Au23	7	38.11	8.047	8.790	1.654	2.502
Au24	24	60.13	7.503	8.629	2.970	2.788
Au27	25	35.91	7.598	8.170	0.852	1.390

- For each Sagittarius analogue, we choose the Solar position which places the Galactic center and the Sagittarius analogue at the correct (within 1 degree) on-sky locations.

Enhancement factors

- Modifications factors when including the unbound DM particle in the calculation of the J-factors for Sagittarius analogues ($\mathscr{J}_{\rm bound+unbound}/\mathscr{J}_{\rm bound}$):

Host name	Dwarf	Sommerfeld	S-wave	P-wave	D-wave
Au16	9	1.14	1.17	20.52	1735.28
Au21	10	1.05	1.04	2.36	45.37
Au23	4	1.04	1.03	3.83	154.27
Au23	7	1.13	1.08	8.33	759.10
Au24	24	1.18	1.22	26.61	3126.15
Au27	25	1.14	1.23	38.34	9765.11

Sagittarius - Fits to gamma-ray data

- The observed gamma-ray source has an extension of $\lesssim 1^{\circ}$.

- Create gamma-ray flux maps using the J-factor maps of the Sagittarius analogues and test them against the data.

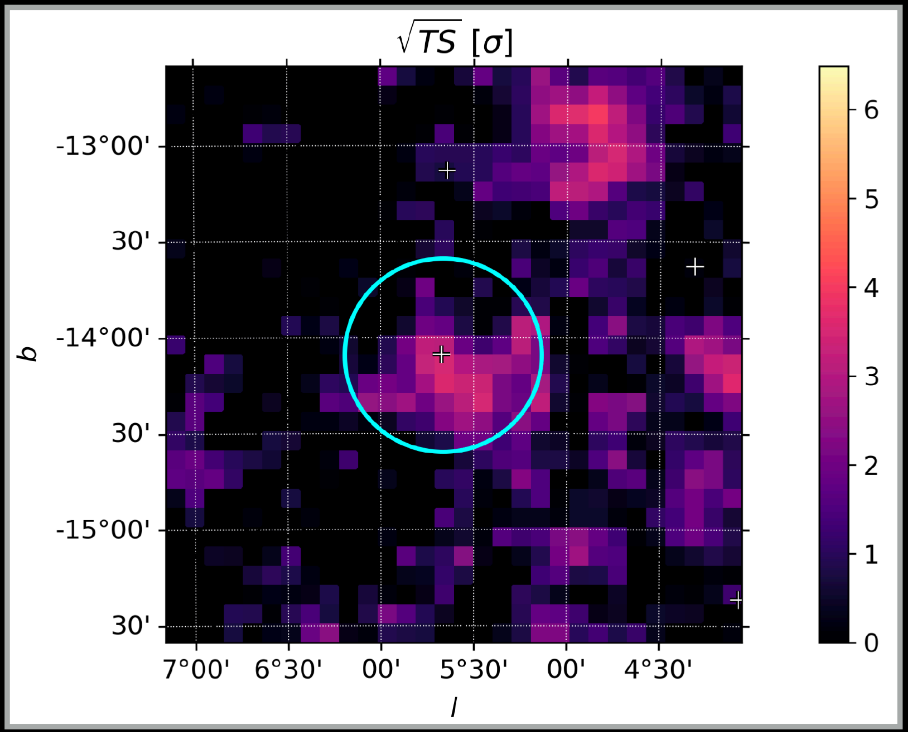

Evans et al., MNRS 524, 3, 4574 (2023)

- Due to the angular extension of our Sagittarius analogues ($\sim 1^{\circ} - 3^{\circ}$), our templates do not provide as good a fit to the gamma-ray data as a simpler point source model.

Sagittarius - DM interpretation

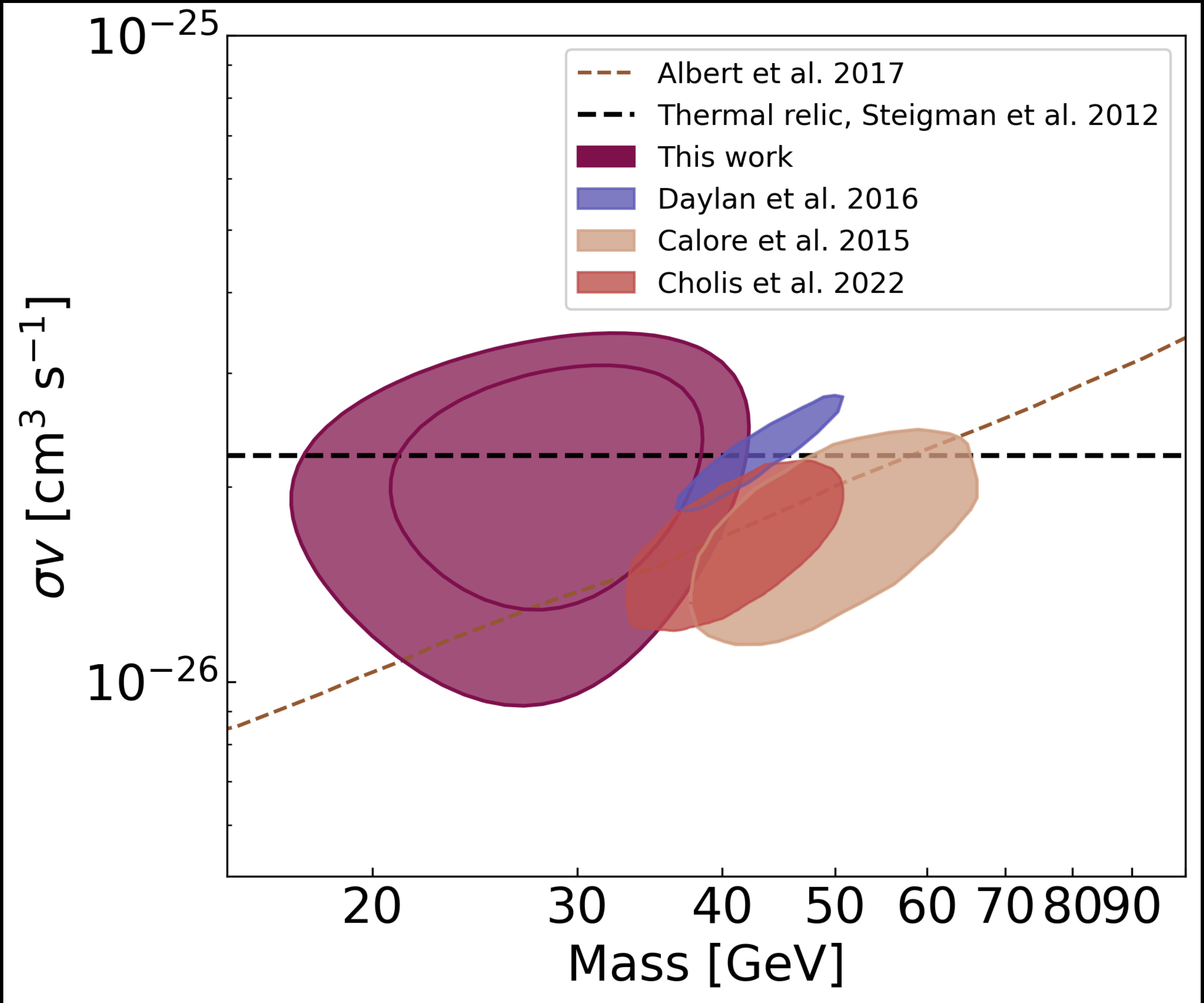

Evans et al., MNRS 524, 3, 4574 (2023)